

Republic of Iraq
Ministry of Higher Education and Scientific Research
AL-Nahrain University
College of Science
Physics Department



Pspice Battery Model with Bidirectional Charging Converter

A Thesis

Submitted to the College of Science of Al-Nahrain
University in Partial Fulfillment of the Requirements
for the Degree of

**Master of Science
In**

Physics

By

Zeena Mowafaq Al-Azzawi
(B.Sc.2004)

Supervised by

Dr. Zainab M. Younis Kubba

In

**Shawal
October**

**1429 A. H.
2008 A.D**

بِسْمِ اللَّهِ الرَّحْمَنِ الرَّحِيمِ

وَعَلَّمَكَ مَا لَمْ تَكُنْ تَعْلَمُ

وَكَانَ فَضْلُ اللَّهِ عَلَيْكَ عَظِيمًا

صدق الله العظيم

سورة النساء

آية (113)

Examination Committee Certification

We certify that we have read the thesis entitled "*Pspice Battery Model with Bidirectional Charging Converter*" and as an examination committee, examined the student *Ms. Zeena Mowafaq Kadury Al-Azzawi* on its contents, and that in our opinion it is adequate for the partial fulfillment of the requirements of the degree of **Master of Science in Physics**.

Signature:

Name: **Dr. Kader H. Al-Shara**

Title: **Assistant Professor**

(Chairman)

Date: / /2009

Signature:

Name: **Dr. Safa Saod Mahdi**

Title: **Assistant Professor**

(Member)

Date: / /2009

Signature:

Name: **Dr. Khalid A. Yahya**

Title: **Lecture**

(Member)

Date: / /2009

Signature:

Name: **Dr. Zainab M. Kubba**

Title: **Lecture**

(Supervisor)

Date: / /2009

Approved by the College Committee of Postgraduate studies

Signature:

Name: **Dr. LAITH ABDUL AZIZ AL- ANI**

Title: **Assistant Professor**

(Dean of the College of Science)

Date: / /2009

Certification

I certify that this thesis entitled “*Pspice Battery Model with Bidirectional Charging Converter*” is prepared by *Ms. Zeena Mowafaq Kadury Al-Azzawi* under my supervision at the College of Science of Al-Nahrain University in partial fulfillment of the requirements for the degree of **Master of Science in Physics**.

Supervisor: Dr. Zainab M. Kubba

Date: 14/10/2008

In view of the recommendations, I present this thesis for debate by the examination committee.

Dr. Ahmad K. Ahmad

Title: Assistant Professor

Head of Physics Department

Date: 14 /10 /2008

DEDICATED
TO
MY PARENTS
AND
BROTHERS

Acknowledgments

Praise be to ALLAH, Lord of the whole creation and peace be upon his messenger Mohammad.

I would like to express my sincere thanks and deep gratitude to my supervisors Dr. Zainab M. Younis Kubba for suggesting the present project of research, and for helpful comments and simulating discussions throughout the research.

I am most grateful to the Dean of College of Science and Head and the staff of the Department of Physics at Al-Nahrain University for their valuable support and cooperation.

Finally, I acknowledge the helpful comments assistance given to me at various stage of this work by Dr. Nahida Jouma AL-Mashhadani. I most grateful to my Parents, my brothers Ahmad, Ali, Mohammad, Omar, Baker for their patience and encouragement throughout this work, and my friends manar majed, Fatma Nafaa, Noor mohammed, for their encouragement.

Zeena

Abstract

This research intends to design Bidirectional Converter that can be used in wide applications from uninterrupted power supplies (UPS), photovoltaic (PV) and battery charging and discharging system, to auxiliary power supplies designed primarily with a general module depending on Orcad PSPICE program.

Lead Acid battery model (12V) is putted, which is used in wide applications. The model consists of charge efficiency and battery voltage components. The charge efficiency factor can vary from (0 to 1) and is dependent on the Battery State of charge and charge current. The voltage component of the model consists of amp-hour integrator which tracks the net current flowing into the battery terminal (Battery voltage). The output of the integrator gives us the state of charge so, it is connected to a table driven voltage source, ETABLE, which generates the equivalent open circuit battery voltage. The method used here is implemented in orcad PSPICE program with bidirectional converter of properties ($D=0.4$, $P=12W$, $V_o=12V$, $f=1\text{ KHz}$, $I_o=1A$).

Contents

Acknowledgments.....IV
Abstract.....V
Contents.....VI
List of Symbols..... IX

Chapter One

Introduction.....1
1.1 Motivation.....1
1.2 Battery.....3
1.3 Lead Acid Battery.....4
1.4 Battery performance characteristics.....5
1.5 Ideal and Non Ideal properties.....7
1.6 Pspice9
1.7 Letrature Servey.....9
1.8 Aim of project.....12
1.9 Thesis overview.....13

Chapter Two

Theory of batteries and Buck-Boost Converter14
2.1 Lead-Acid battery14
2.2 State of Charge (SOC) Determination16
2.2.1 Direct Measurement.....17

2.2.2 Voltage-based SOC Estimation.....	18
2.2.3 Current-based SOC Estimation.....	18
2.2.4 Specific gravity Method.....	19
2.3 Charge Efficiency	20
2.4 DC-DC Switch Mode Converters	20
2.4.1 Control of DC-DC Converters.....	21
2.4.2 Buck-Boost Bidirectional Converter.....	23
2.4.3 Selection of inductance	26

Chapter Three

<i>Design, Modeling and Simulation.....</i>	<i>28</i>
3.1 Introduction.....	28
3.2 Lead-Acid battery PSPICE Model.....	28
3.2.1 Charge efficiency Factor.....	29
3.2.2 Battery Voltage Components.....	32
3.3 Converter Circuit Design.....	35
3.4 Pulse Width Modulation (PWM) and Gate Drive Circuit.....	36
3.5 Boot-Strap Circuit Technique (BSCT).....	37

Chapter Four

<i>Results and Discussion.....</i>	<i>39</i>
4.1 Battery model Simulation.....	39
4.2 Analytical Result obtained by PSPICE.....	49
4.3 Bidirectional converter with Battery model results.....	52

Chapter Five

<i>Conclusions and Future Work</i>	59
4.1 Conclusions.....	59
4.2 Future Work.....	59
References	61

<i>List of Symbols</i>	
<i>Symbols</i>	<i>Description</i>
AH	Ampere-Hour
Bat cur	Battery current
C_{batt}	Input Capacitance
C_{bus}	Bus Capacitance
D	Duty cycle
fs	Switching frequency
fld	flooded
i_{bat}	Battery charging current
L	Inductance
Nameplate Capacity	Initial Capacity
R_{int}	Battery internal resistance
R_2	Sum of the inductor's resistance
$S_{initial}$	Initial state of charge
sld	Sealed
t_{on}	time switch on duration
T_s	Total time
Temp C	Temperature ,degC
V_{st}	Saw tooth Voltage
$V_{control}$	Control Voltage (amplified error)

<i>List of abbreviation</i>	
<i>abbreviation</i>	<i>Description</i>
ABM	Analog Behavioral Modeling
BMS	Battery management system
BSCT	Boot Strap Circuit Technique
ESR	Equivalent Series Resistance
HST	Hubble Space Telescope
IGBT	Insulated Gate Bipolar Transistor
MOSFET	Metal Oxide Semiconductor Field Effect Transistor
PSPICE	Personal Simulation Program with Integrated Circuit Emphasis
PWM	Pulse Width Modulation
RC	Resistive Companion
SLA	Sealed Lead Acid
SOC	State of Charge
VRLA	Valve Regulated Lead Acid
VTB	Virtual Test Bed

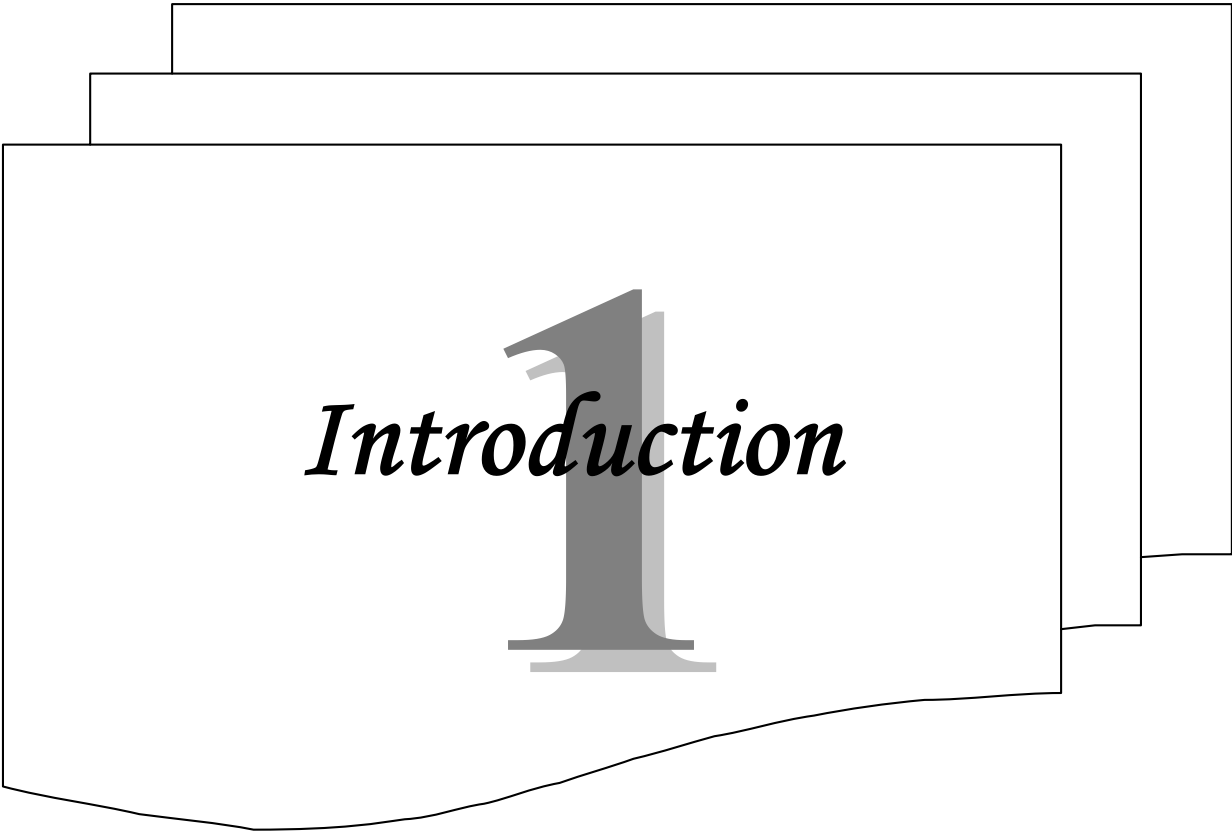
<i>List of Figures</i>		
<i>Figure No.</i>	<i>Caption</i>	<i>Page No.</i>
Figure (1-1)	The proposed power conditioning system block diagram	1
Figure (1-2)	Basic bidirectional switching cells used for constructing multipart bidirectional converters	2
Figure (1-3)	Battery Cell Composition	3
Figure (1-4)	Pb, Pbso4/H2SO4/ PbO2, Pb Cell	5
Figure (1-5)	Characteristics of an ideal battery: constant voltage and constant capacity	7
Figure (1-6)	Non-ideal battery properties	8
Figure (2-1)	Control Circuit of DC-DC Converter	22
Figure (2-2)	Buck Boost converter schematic	23
Figure (2-3)	Current thorough Vbattery ripple waveform	26
Figure (3-1)	Pspice lead-acid battery model	۲۹
Figure (3-2)	r_t three terms as represented by ABM in PSPICE	۳۱
Figure (3-3)	The charge efficiency factor as represented in PSPICE	۳۲
Figure (3-4)	The battery voltage component represented in PSPICE	۳۳
Figure (3-5)	Complete circuit of the battery as Represented in PSPICE	۳۴
Figure (3-6)	Non-Isolated Single-Phase Bidirectional Buck Boost converter	35
Figure (3-7)	The system of the PWM generator and gat drive circuit	۳۷
Figure (3-8)	Complete Circuit of the Converter as Represented in PSPICE	۳۸
Figure (4-1)	Battery voltage as a function of time at different RL (0.1Ω, 0.3Ω, and 0.5Ω)	۴۱
Figure (4-2)	State of charge as a function of time at different RL (0.1 Ω, 0.3 Ω and 0.5 Ω)	۴۱

<i>Figure No.</i>	<i>Caption</i>	
Figure (4-3)	Charge efficiency as a function of time at different RL (0.1 Ω , 0.3 Ω and 0.5 Ω)	३५
Figure (4-4)	battery voltage as a function of state of charge at RL=0.5 Ω	42
Figure (4-5)	Charge efficiency as a function of state of charge at RL=0.5 Ω	43
Figure (4-6)	Battery voltage as a function of time at different Kval (0.1, 0.2 and 0.3)	३५
Figure (4-7)	State of charge as a function of time at different Kval (0.1, 0.2 and 0.3)	३६
Figure (4-8)	Charge efficiency as a function of time at different Kval (0.1, 0.2 and 0.3)	4६
Figure (4-9)	Battery voltage as a function of state of charge at Kval=0.3	३०
Figure (4-10)	Charge efficiency as a function of state of charge at Kval=0.3	4०
Figure (4-11)	Battery voltage as a function of time at different Rbatt (0.066 Ω , 0.086 Ω and 0.106 Ω)	4१
Figure (4-12)	State of charge as a function of time at different Rbatt (0.066 Ω , 0.086 Ω and 0.106 Ω)	4१
Figure (4-13)	Charge efficiency as a function of time at different Rbatt (0.066 Ω , 0.086 Ω and 0.106 Ω)	३५
Figure (4-14)	battery voltage as a function of time at different temperature	4५
Figure (4-15)	State of charge as a function of time at different temperature	३१
Figure (4-16)	Charge efficiency as a function of time at different temperature	4१
Figure (4-17)	Voltage of converter	००
Figure (4-18)	Output Voltage of bidirectional converter	०१
Figure (4-19)	Output Current of bidirectional converter	०१
Figure (4-20)	Total circuit of the battery and converter as represented in PSPICE	०५
Figure (4-21)	Voltage as a function of time	०६
Figure (4-22)	current and battery voltage as a function of time	5०

<i>List of Figures</i>		
<i>Figure No.</i>	<i>Caption</i>	<i>Page No.</i>
Figure (4-23)	Charge efficiency as a function of time	๐๖
Figure (4-24)	Charge efficiency as a function of state of charge	๐๖
Figure (4-25)	State of charge as a function of time	5๗
Figure (4-26)	Battery voltage as a function of state of charge	5๗
Figure (4-27)	State of charge as a function of time at different temperature	๐๘
Figure (4-28)	Charge efficiency as a function of time at different temperature	58

<i>List of Tables</i>		
<i>Table No.</i>	<i>Caption</i>	<i>Page No.</i>
Table (1-1)	Battery characteristics	3
Table (2-1)	Battery specifications	15
Table (3-1)	Parameters of used in equations for Lead acid battery	30

Chapter
One



Introduction

1

Chapter One

Introduction

1.1 Motivation

There are many applications for bidirectional DC-DC converters ranging from spacecraft to renewable energy applications such as electric vehicles and fuel cell power generation. Each of these applications requires specific attention to be paid to cost, performance and reliability with fuel cell energy management systems being no different. [Andy 2003]

The entire power conditioning system is divided into three main sections: (1) the dc-dc converter that boosts from the (fuel cell, solar cell.....etc) to the high voltage bus, (2) the dc-ac inverter, (3) the auxiliary energy management system that consists of a battery bank and a bidirectional dc-dc converter to provide power during load transients. Figure (1-1) shows the block diagram of the proposed power conditioning system. [Chris.S and et al 2003]

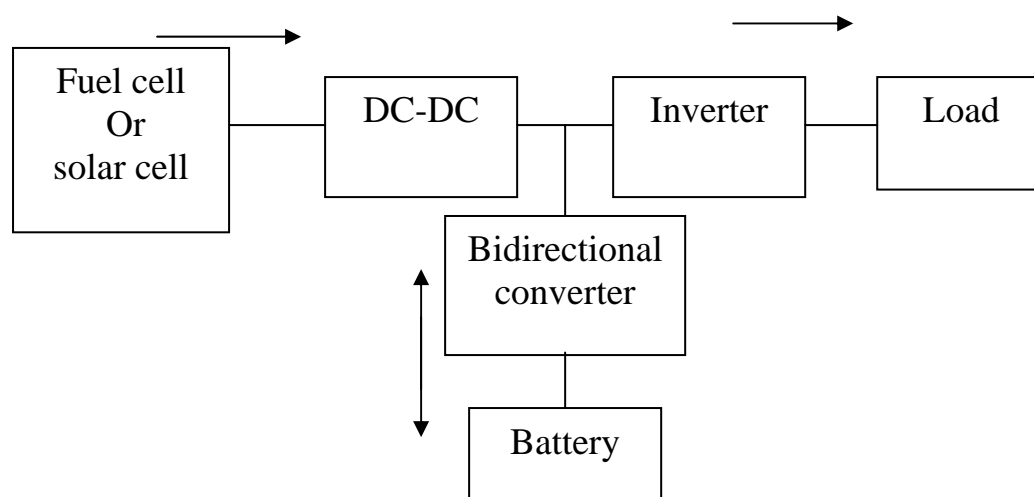


Figure (1-1) the proposed power conditioning system block diagram [Chris.S and et al 2003]

Higher voltage batteries could be directly connected to the dc link without any intermediate power converter, but the high voltage battery is relatively expensive and may have the battery cell unbalance problem in the long run. A battery pack is connected to the dc link via a bi-directional Dc-Dc converter. [Jinhee lee and et al 2003]. In some applications, such as battery charging and discharging, it is desirable to have bidirectional power flow capability.

Bidirectional Boost converters can be classified as isolated and no isolated. There are three main converters that can be used on either side of the transformer, push-pull, full-bridge or half-bridge and can be either current or voltage fed. Of these, only certain combinations are cost-effective and efficient depending on their placement, either on the low or high side. [Andy 2003] A multipart bidirectional converter can be constructed from the basic bidirectional switching cell as shown in figure (1-2). Using interleaved topologies, the proposed basic cells can also be used for high-power applications. [Haimin Tao]

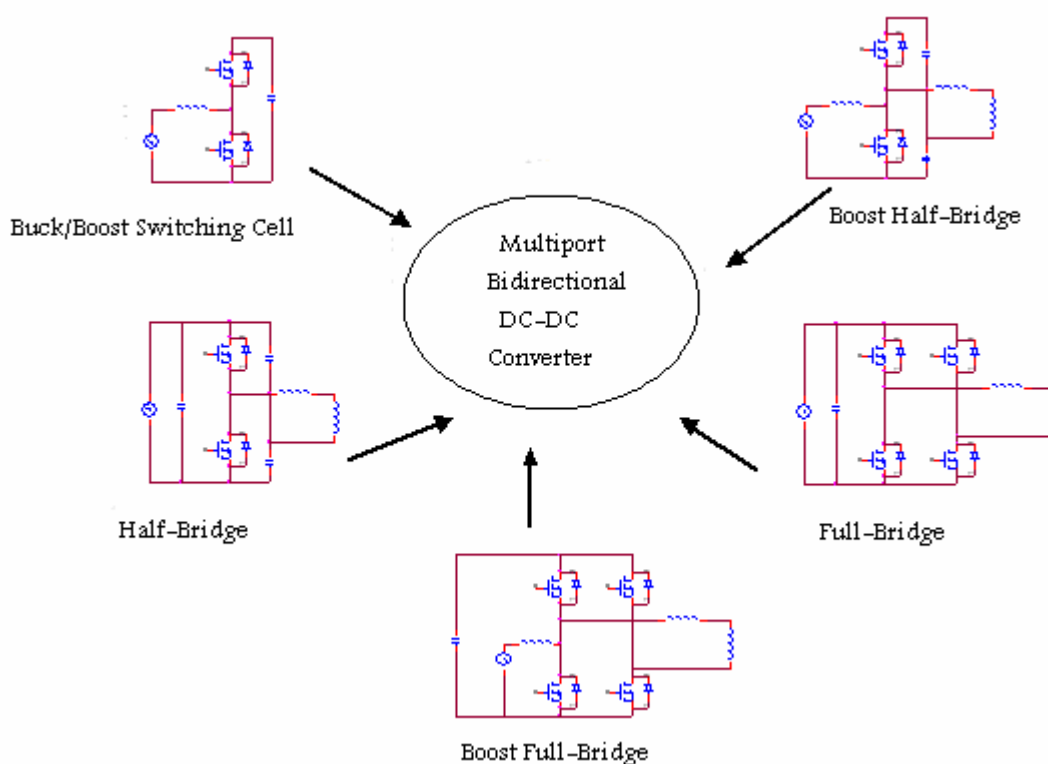


Figure (1-2) Basic bidirectional switching cells used for constructing multipart bidirectional converters [Haimin Tao]

1.2 Battery

A battery is a device that converts chemical energy directly to electrical energy. It consists of one or more voltaic cell. Each voltaic cell consist of two half cells connected in series by a conductive electrolyte. Each cell has a positive electrode (cathode), and a negative electrode (anode). These do not touch each other but are immersed in a solid or liquid electrolyte. In a practical cell the materials are enclosed in a container, and a separator between the electrodes to prevent the electrodes from coming into contact as shown in figure (1-3). **[Battery electricity 2007]**

Many types and classifications of batteries are manufactured today. Each, with specific design and performance characteristics suited for particular applications. Table (1-1) summarizes some of the key characteristics of the different battery types as shown in appendix (B). **[James 1997]**

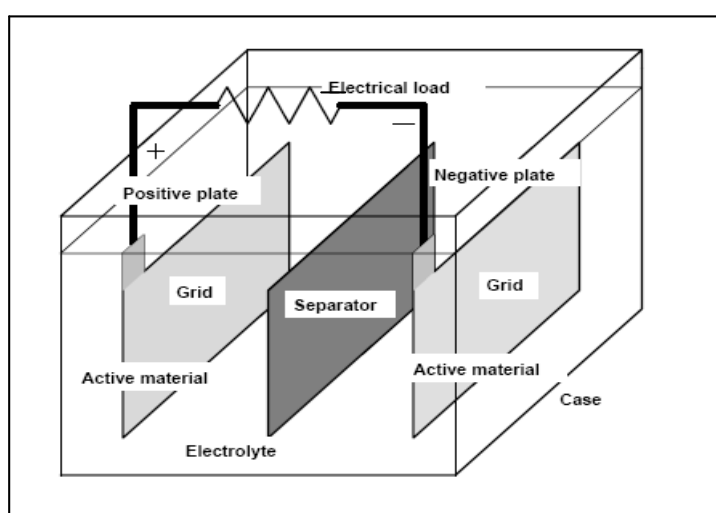


Figure (1-3) Battery Cell Composition [James 1997]

1.3 Lead Acid Battery

Most economical for large power application where weight is of little concern. The lead acid battery is preferred choice for hospital equipment, wheelchairs, emergency lighting and ups system. [Isidor 2001]

This type is used to validate the PSPICE model so all details of this type will be discussed.

Let us consider a cell such as shown in figure (1-4). This cell schematically represents a classic Lead-acid battery. It consists of a lead electrode (pb) and another of lead oxide (PbO₂) submerged in an H₂SO₄ solution. When the two electrodes come together figure (1-4a), an electric current flows from one to the other due to an electrostatic potential difference between the two electrodes. The reaction giving rise to this electromotive force is



This reaction can be split into two parts. One that takes place in the left electrode,



And the other that takes place in the right one,



If a potential greater than its electromotive force is applied to the cell, the chemical process is inverted in the electrodes figure (1-4b) and the direction of the reaction (1-2) and (1-3) is also inverted. The pb electrode is transformed into the cathode and the PbO₂ into the anode, with the system now working as an electrolytic cell. [Esperilla.J.J and et al 2006]

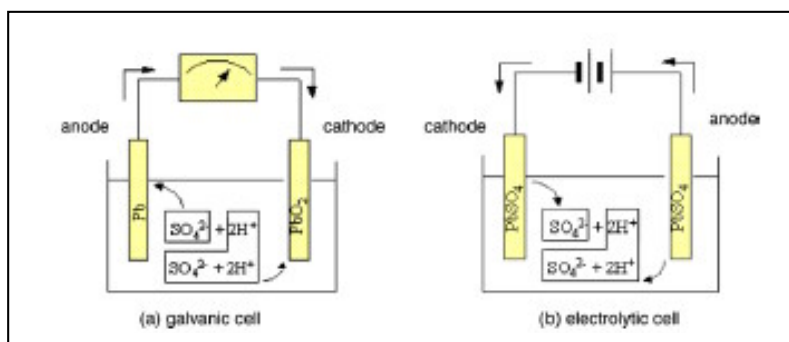


Figure (1-4) Pb, Pbso4/H2SO4/ PbO2, Pb Cell [Esperilla.J.J et al 2006]

1.4 Battery performance characteristics

Ambient Temperature

The prevailing surface temperature to which a battery is exposed.

Capacity

The electrical energy available from a cell or battery expressed in ampere-hours. Available capacity refers to ampere-hours that can be discharged from a battery based on its state of charge, rate of discharge, ambient temperature, and specified cut-off voltage. Rated capacity (“C”) is the discharge capacity that the manufacturer says may be obtained at a given discharge rate and temperature.

[Ruffin Rd and San Diego 2004]

Rated Charge Capacity

The capacity, usually given in ampere-hours (Ah) or milliamper-hours (mAh), specified by the manufacturer and typically printed on the label of the battery itself. If a batch of batteries includes parallel connections, the rated charge capacity of the batch is the total charge capacity of the parallel configuration, that is, the rated charge capacity of each battery time the number of batteries connected in parallel. Connecting multiple batteries in series does not affect the rated charge capacity. [Suzanne Foster Porter 2008]

Discharge

The process of drawing current from a battery. Deep Discharge – the discharge of a cell or battery to between 80% and 100% of rated capacity. Depth of Discharge – the amount of capacity – typically expressed as a percentage – removed during discharge. Self Discharge – the loss of capacity while stored or not in use. Self Discharge Rate – the percent of capacity lost on open circuit Over a specified period of time.

Impedance

The (resistive and reactive) value of a battery to an AC current expressed in ohms (Ω). Generally measured at 1000 Hz at full charge.

Internal Resistance

The resistance inside a battery which creates a voltage drop in proportion to the current draw.

Open Circuit Voltage

The voltage of a battery or cell when measured at no load condition.

State of Charge

The available capacity of a battery at a given time expressed as a percentage of rated capacity. Discharging a battery results in a decrease in state of charge, while charging results in an increase in state of charge.

Thermal Runaway

A condition in which a cell or battery on constant potential charge can destroy itself through internal heat generation. **[Ruffin Rd and San Diego 2004]**

1.5 Ideal and Non Ideal properties

The two most important properties of batteries from the viewpoint of some one using them are voltage and capacity. An ideal battery has a constant voltage throughout a discharge, which drops instantaneously to zero when the battery is fully discharge and has constant capacity no matter what is the rate of the load as shown in figure (1-5). [**Thomas and Daniel 1999**]

While ideally a battery has constant voltage and capacity, in practice both vary widely. Figure (1-6a). Shows the battery voltage as a function of discharge time for two different loads. The load on the battery for discharge curve (1) is smaller than load for discharge curve (2). The capacity also varies with the value of the load figure (1-6b). Shows the loss of capacity with increasing load current for a typically NiCd battery. The second non-ideal capacity property, recovery is shown in figure (1-6c). A reduction of the load for a period of time results in an increase in battery capacity. [**Kubba Z.M 2003**]

Figure (1-5) Characteristics of an ideal battery: constant voltage and constant capacity

[Thomas and Daniel 1999]

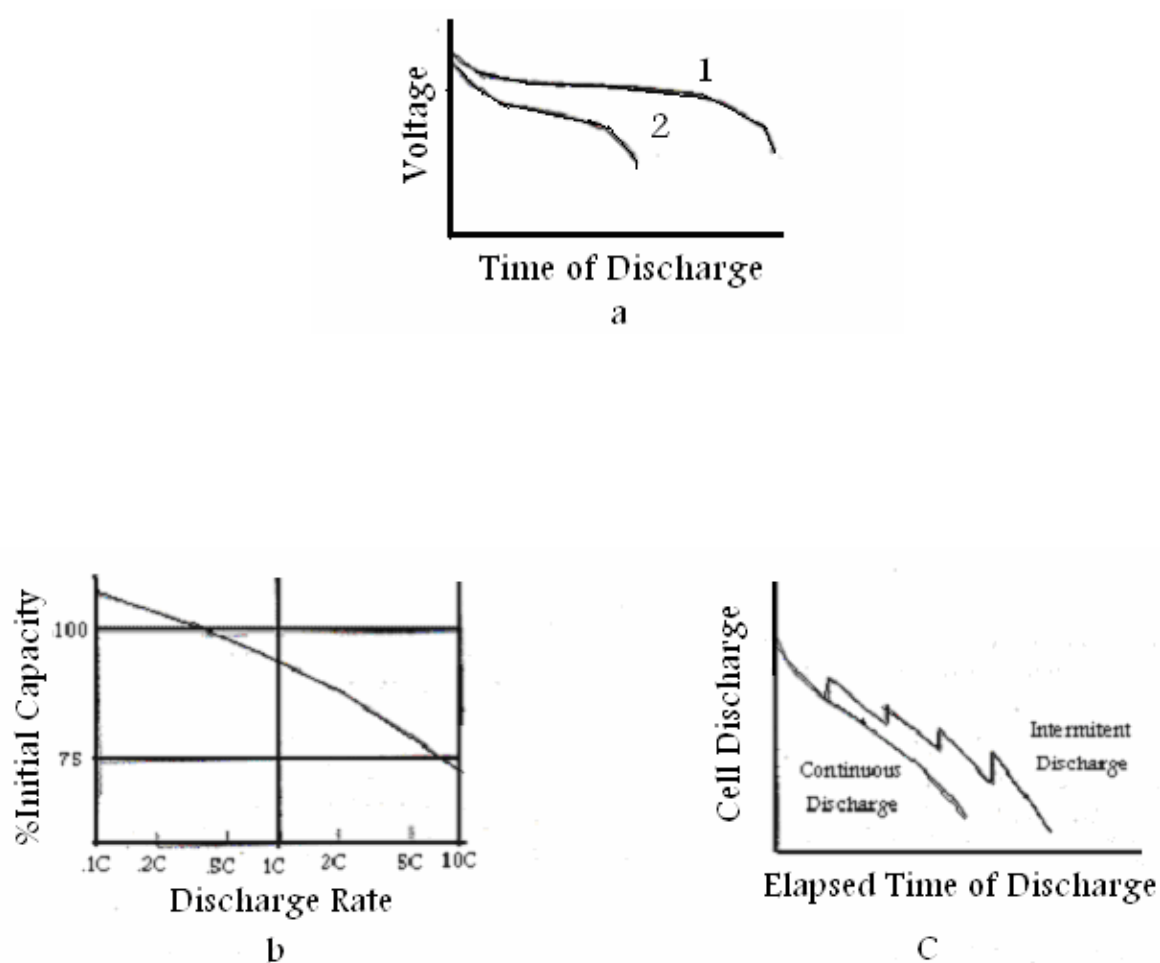


Figure (1-6) Non-ideal battery properties:

- (a) Voltage change,
- (b) Loss of capacity, and
- (c) Recovery [zainab 2003]

1.6 Pspice

There are several circuit simulation programs available on the market such as SPICE, EMTP and SABER among several others. In this a spice simulator is used, pspice.

A spice stands for simulation program with integrated circuit emphasis. The language was developed at the University of California, Berkley. Spice is a language developed for simulation integrated circuits. [Mikael 2007]

1.7 Letrature Servey



A Voltaic Pile, the first modern battery.

More often than not, battery performance in a particular device is still determined by testing. Testing, although time-consuming and expensive, is necessary because the performance of a battery depends on how the battery is used. However, advances in computer simulation of battery performance now allow good estimates of battery performance to be made, so devices can be designed in software.

R.Tim and H.John, in 1994 are described an electrical model of a battery that can accurately simulates characteristic battery behavior during over-current instances using the analog bahavioural modeled functions available with Micro Sim's PSpice simulation software. . The battery model can be coupled with other distribution component models to simulate the protection performance in telecommunication Dc distribution system. **[Tim.R and John.H 1994]**

B.Wu, and et al, in 2001 are described Resistive Companion (RC) modeling in an easy-to-use approach for electric circuit simulations. With a RC numerical solver, simulations of complex electric system can be achieved based on RC models. In this study, the construction of RC battery models is investigated. A general battery model and a nickel-metal hydride cell model have been built. Simulations of RC battery models on Virtual Test Bed (VTB) are presented and analyzed. It is shown that RC modeling provides a flexible and powerful way for the simulation of battery systems. **[Wu.B and et al 2001]**

F.A.Himmelstoss and P.A.Wurm , in 2002 they used tapped inductors and current bi-directional switches in the classical boost or buck-boost converter leads to a high step-up ratio, thus avoiding the extreme duty cycles of the active switches and the high stress switches. A high Voltage DC-link and a battery of low voltage can therefore be coupled easily. Due to the possibility of bidirectional power flow charging and discharging of the battery is possible. Two converters are presented and analyzed. Due to the simultaneous regulation of the switching frequency and the duty cycle on one hand and the winding ratio of an autotransformer on the other, high conversion rates of 1:5 can easily be realized. The dimensioning of the converters, their dynamical behavior, and the component stresses are analyzed. **[Himmelstoss.F.A and Wurm.P.A 2002]**

M. Hashem Nehrir, and et al, in 2002 is presented the development of a computer approach for evaluating the general performance of stand-alone

wind/photovoltaic generating systems. Simple models for different system components are developed, integrated, and used to predict the behavior of generating systems based on available wind/solar and load data. The model is useful for evaluating the performance of stand-alone generating systems and gaining a better insight in the component sizes needed before they are built. **[Hashem Nehrir.M and et al 2002]**

S. Abu-Sharkh and D.Doerffel, in 2005 described battery model for a high power Lithium-Ion battery. An IsSpice4 model was made using the techniques and data described, and it was scaled down for use with a C cell (1.4 amp-hr, 3.6 volt). They described the batteries that hold their charge for many hours, making a PSPICE simulation impossible over the entire charge-discharge cycle when other circuit operations need to be simulated. Time constants on the order of seconds are long enough to appear to be steady state for surrounding circuitry, and are short enough to run simulations without running out of memory. **[Issue#78, November 2005]**

J.J Esperilla, and et al, 2006 presented a model of a lead-acid battery developed with bond graphs. The bond graph structure was used to reproduce the behavior of reversible electrochemical cell in charging condition or in discharging conditions. The charging process for a standard 12V battery for two different voltage charges was simulated using both isothermal model and the thermal model. With the later, it was seen that when the charge currents are high, the thermal effects are considerable, and at the end of the charge process the electrolyte reaches temperatures considerably higher than at the beginning. This increase in electrolyte temperature has repercussions on the charge current value, and as a result, on the State of Charge (SOC). **[Esperilla.J.J and et al 2006]**

M.Thele and et al, 2006 presented a model for flooded and VRLA batteries that is parameterized by impedance spectroscopy and includes the overcharging effects

to allow charge-acceptance simulations (e.g. for regenerative braking drive-cycle profiles). The full dynamic behavior and the short-term charge/discharge history are taken into account. This is achieved by a detailed modeling of the sulfate crystal growth and modeling of the internal gas recombination cycle. The validation measurements have been performed for different types of Lead-acid batteries (flooded and VRLA). The complete battery model allows for charge-acceptance tests which are a prerequisite for the development of complex electrical systems such as vehicles with regenerative-braking. [Thele.M and et al 2006]

E. Sanchis-Kilders, in 2006 are presented the results of a project that looked after a high efficiency bidirectional converter which could be used as a battery discharge/charge regulator when the bus voltage is above the battery voltage. High efficiency, high stability and simplicity are the main goals, no galvanic isolation is required. Taking into account all these parameters, a new topology based on a Boost converter with coupled inductors has been proposed. The use of a bidirectional converter reduces the mass of the overall charge/discharge subsystem and lowers cost and component count. [Sanchis-Kilders.E et al 2006]

1.8 Aim of project

This thesis provides theoretical studies to build battery modeling techniques of type Lead-acid battery using charge efficiency and battery voltage components. After modeling and simulating the battery model, it will be considered as an auxiliary source to the Bidirectional Buck-Boost Converter in order to test the battery model validity.

1.9 Thesis overview

The work deal mostly with the modeling and simulating of a lead acid battery as well as an Bidirectional converter charger.

Chapter one presented the introduction including the Bidirectional converter principles, battery types, battery performance characteristics and the previous work was presented to show the extent of research interest in this field.

Chapter two describes the principles of single phase Bidirectional converter. A paragraph is also included detailing the parameters of the battery (SOC, internal resistance and charge efficiency).

Chapter three

Chapter four discusses the development and simulating results of a battery model and Bidirectional converter using Pspice circuit simulation software.

Finally Chapter five gives the conclusions and suggestion to continue and to extend this work in the future.

Chapter
Two

*Theory of batteries and Buck-
Boost Converter*

Chapter Two

Theory of batteries and Buck-Boost Converter

2.1 Lead-Acid Battery

In 1859 a French physicist Gaston Planté, Invented the oldest type of rechargeable battery. Despite having the second lowest energy-to-weight ratio (next to the nickel-iron battery) and a correspondingly low energy-to-volume ratio, their ability to supply high surge currents means that the cells maintain a relatively large power-to-weight ratio. These features, along with their low cost, make them attractive for use in cars, as they can provide the high current required by automobile starter motors. They are also used in vehicles such as forklifts, in which the low energy-to-weight ratio may in fact be considered a benefit since the battery can be used as a counterweight. Large arrays of lead-acid cells are used as standby power sources for telecommunications facilities, generating stations, and computer data centers. They are also used to power the electric motors in diesel-electric (conventional) submarines. Table (2-1) summarizes of the key specifications of Lead acid battery. **[Lead-acid battery 2006]**

In terms of numbers of units or of watt-hours of capacity, the usage of the lead-acid battery is probably over twenty times as that as large as that of its nearest rival, the nickel-cadmium (or ion) alkaline storage battery. **[KADHEM.M .S 1995]** There are several contributory factors to this success:

- (a) Great versatility; the battery can supply on instant demand high or low currents over a wide range of temperatures.
- (b) Good storage characteristics, particularly in the dry-charged condition.
- (c) A very high degree of reversibility: It is capable of giving hundreds of discharge-charge cycle with great reliability.
- (d) Lead, the basic material of construction, has a low melting point and the various metallic components, grid , bus bars, terminal posts, inter-cell connectors. Can be easily coated and grouped together by simple low temperature welding techniques.
- (e) High cell voltage, due to high potential of the lead dioxide electrode in sulfuric acid, namely $E=1.685V$, gives a cell voltage of 2.04V.
- (f) The metal is relatively cheap, when compared with nickel, cadmium and silver used in other storage batteries.

Table (2-1) Battery specifications [Lead-acid battery 2006]

Parameters	Value
Energy/weight	30-40 wh/kg
Energy/size	60-75 wh/L
Power/Weight	180 W/kg
Charge/discharge efficiency	70%-92%
Energy/consumer price	7(sld)-18(fld) wh/Us\$
Self-discharge rate time durability	3%-20%/month
Cycle durability	500-800 cycles
Nominal Cell Voltage Charge temperature interval	2.0 V

Driven by different application, two battery designations emerged. They are the small Sealed Lead Acid (SLA); also known under the brand name of Gel cell, and large Valve Regulated Lead Acid (VRLA).

Unlike the flooded Lead acid battery, both the SLA and VRLA are designed with a low over-voltage potential to prohibit the battery from reaching its gas-generating potential during charge excess charging would cause gassing and water depletion. Consequently, these batteries can never be charged to their full potential. **[Isidor 2001]**

The most common type used is the Valve Regulated Lead Acid (VRLA) battery, because of its low cost, maintenance-free operation and high efficiency characteristics. **[Koutroulis, E., and Kalaitzakis, K. 2004]**

2.2 State of Charge (SOC) Determination

The state of charge of a battery is useful in determining the available capacity of the battery. It is expressed as the percentage of the rated capacity of the battery. State of charge tells the user how much more energy the battery can deliver to the application before it needs recharging. A Battery Management System (BMS) should determine the SOC of individual cells in a battery pack to check for uniform distribution of SOC among the cells. Usually the SOC is expressed as a percentage of the rated capacity, rather than of the capacity to which the battery was last charged. The rated capacity of the cell is not the same as the capacity of the battery to which it was last charged because of aging and environmental effects that prevent the battery from charging to its rated

capacity as time passes. However, if the SOC is used only for cell equalization purposes, it can be expressed either way, as all the cells in a string generally experience the same environment.

It is not possible to measure the SOC of a battery directly therefore, a physical parameter that varies with the SOC is measured to determine the SOC of a battery. Based on the physical parameter that is measured, SOC determination methods are classified into the following types:

1. Direct Measurement
2. Voltage-Based SOC Estimation
3. Current-Based SOC Estimation
4. Specific Gravity Method

Each of these methods is now described in more detail.

2.2.1 Direct Measurement

The direct measurement method for SOC assumes that the current through the cell is constant. The state of charge is calculated solely in terms of the elapsed time, based on $\Delta q = i\Delta t$. The controller that is being used to calculate the SOC of the charging and discharging process and accumulates time either positively or negatively to determine the SOC. This method has two problems associated with it. First, this method requires that the current through the battery is to be constant. The current through a battery in fact is not constant; it increases/decreases as the battery charges/discharges, in a nonlinear fashion. Therefore, a more accurate measure would require that actual current be measured and accumulated over time. Second, this method requires that the battery is to be discharged in order to determine how much charge it contained initially. [Annavajjula V.K 2007]

The SOC could be measured simply by integrating the battery charging current i_{bat} as follows, [Jinhee lee et al 2003]

$$\text{SOC} = \frac{Q_0 - \int i_{\text{bat}} dt}{Q_n} \quad (2-1)$$

where Q_0 is initial charge and Q_n is rated ampere-hour of battery. The initial charge Q_0 is set to be Q_n when the system starts from full battery charge. [Jinhee lee et al 2003]

2.2.2 Voltage-based SOC Estimation

This method is applicable to cell chemistries whose voltages are directly proportional to the available state of charge. [Annavaajjula V.K 2007]

$$V_{\text{oc}}(t) = a_1 * \text{SOC}(t) + a_0$$

$$\text{SOC}(t) = \frac{V_{\text{oc}}(t) - a_0}{a_1} \quad (2-2)$$

where SOC (t) is the stat of charge of the battery, a_0 is the battery terminal voltage, a_1 is the obtained knowing the value of a_0 and V_{oc} .

If this relation is known a priori, the SOC can be obtained by measuring the open circuit voltage. In practice, the SOC varies widely with temperature, discharge rate and aging of the battery; all these factors must be considered for an accurate determination of SOC.

2.2.3 Current-Based SOC Estimation

Like direct measurement, current-based SOC estimation uses the basic definition of the charge $q = \int_0^t i(t) dt$ to determine the SOC of a battery;

charge is obtained by integrating the current. This method accumulates the current drawn in and out of the battery over time to determine the capacity of the battery. Therefore, this method is also known as Coulomb counting. The current flowing in and out of the battery is obtained by measuring the voltage drop across a known low ohmic, high precision, series resistor. [Annavaajjula V.K 2007] In coulomb method, SOC is estimated by subtracting charge flow out of battery from the initial existing charge as described by this eq. [Sauradip M. 2001]

$$\text{SOC} = S_{\text{initial}} - \text{Charge flow out of battery} \quad (2-3)$$

S_{initial} is initial state of charge of battery (i.e. before discharge takes place, if battery is full charge $S_{\text{initial}}=100$). However, the non-linear and time varying behavior of battery poses a severe problem with the coulomb metric method. As for example, a battery of capacity C A-h at C/20 rate would suggest different capacities with different discharge rates. The capacity of battery is also a function of battery temperature. Also a battery displays a variation in performance with aging and other operational factors (Charging pattern, Depth of Discharge). [Sauradip M. 2001]

2.2.4 Specific Gravity Method

Specific gravity is the ratio of the weight of a solution to the weight of an equal volume of water at a specified temperature. Specific gravity is used as an indicator of the state of charge of a cell or battery. However, specific gravity measurements cannot determine a battery's capacity. [John A. Yoder 1995]

2.3 Charge Efficiency

Charge efficiency refers to how many amp-hours are absorbed by the battery compared to how many charge amp-hours are delivered. **[Blue Sky Energy Inc 2004]**

2.4 DC-DC Switch Mode Converters

A switch mode DC-to-DC converter is used to convert the unregulated DC input into controlled DC output at a desired voltage level. This converter is very often used in conjunction with a transformer for electrical isolation in DC power supplies and most often without isolation in DC motor drives. There are five major types of DC-DC switch mode converters. The two basic converter topologies are the step down (buck) converter and the step up (boost) converter. From the combination of these two basic topologies are the buck-boost converter and the Cuk converter. The last one is the full bridge and half bridge converter, which is derived from a step-down converter. Unlike the other four this converter has the ability to be operated as an inverter since the power could be manipulated in a bi-directional manner. This converter is commonly used for DC Motor drives and to convert DC to AC as an inverter. In analysing the four converters mentioned, the following assumptions were considered; the converters are in steady state condition, the switches are ideal (lossless), the DC input have zero internal impedance however in most cases the input is a diode rectified AC line voltage with a large filter capacitor, to provide a low internal impedance and a low ripple DC voltage output and at the load side a small filter is treated as an integral part of the converter. **[Mohan N. 1989]**

2.4.1 Control of DC-DC Converters

The control of the DC-DC converter could be accomplished by injecting a Pulse Width Modulated (PWM) signal in the gate of the power electronic switch. This switch can be a MOSFET or an IGBT. The PWM could either be varied by altering the time in which the pulse is at high or low position and by altering both the period of the PWM signal and the time in which it is “on” or “off”. The second method however makes it complicated to filter the input and output ripple component of the waveform in the converter. For the first method the PWM signal needed for controlling the “on” and “off” position of the switch is generated by comparing a repetitive triangular waveform with a control signal voltage shown in figure (2-1). The switching frequency is determined by the frequency of the constant peak repetitive triangular waveform. For the control voltage it is generated by amplifying the error signal of the converter output and the desired voltage level. Base on figure (2-1) when the instantaneous value of the triangular waveform is greater than the control voltage the pulse is at its low position hence the switch will be close. When it is lesser than the control voltage the pulse is at its high position closing the switch. The duty cycle of the switch can be related by the ratio of the control voltage magnitude and the peak value of the repetitive waveform. In terms of V_{control} and the peak of the saw tooth waveform V_{st} , the switch duty ratio can be expressed as: **[Mohan N. 1989]**

$$D = \frac{t_{\text{on}}}{T_s} = \frac{V_{\text{control}}}{V_{\text{st}}}$$

where

t_{on} : time switch on duration

T_s : total time

V_{st} : Saw tooth Voltage

$V_{control}$: Control Voltage (amplified error)

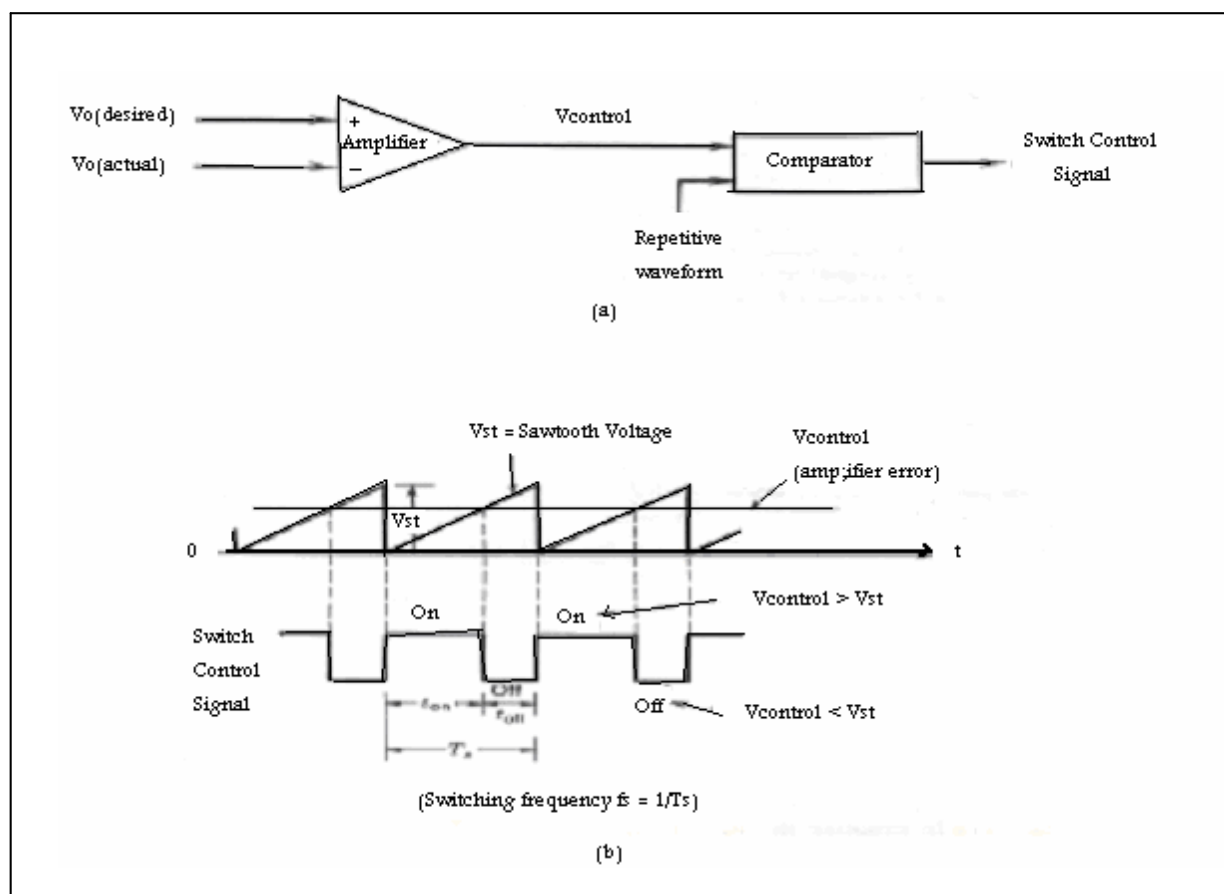


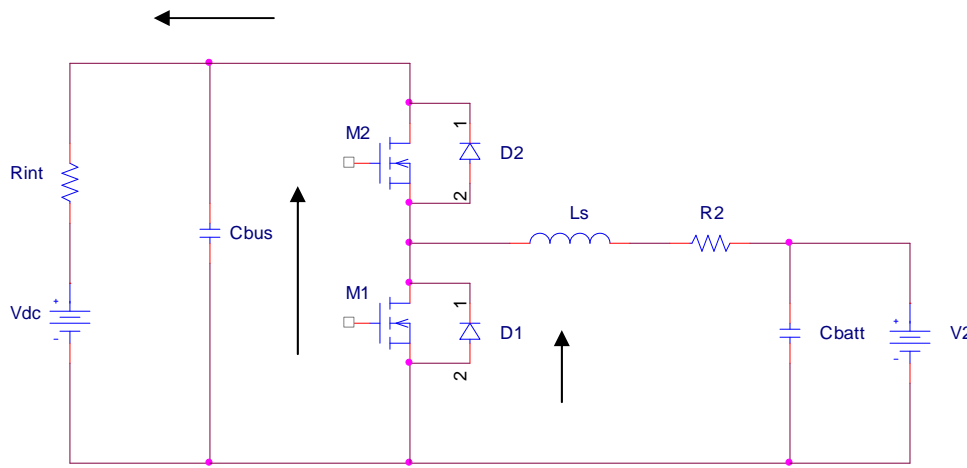
Figure (2-1) Control Circuit of DC-DC Converter [Mohan N. 1989]

(a) Block Diagram

(b) Comparator Signal

2.4.2 Buck-Boost Bidirectional Converter

A buck-boost bidirectional converter is the simplest topology and contains two active switches and a single inductor. In boost mode the switch must carry the full power and likewise for the inductor. This requires the devices and magnetics to be quite large. [Andy M. 2003]



Figure(2-2) Buck Boost converter schematic [Micah Ortuzar et al 2003]

Figure (2-2) shows a simplified schematic of the Buck-Boost converter and the two connected sources. The V_{battery} bank is considered as a constant voltage source (V_2) with a series resistance and (V_{dc}) as an ideal voltage source with its internal series resistance.

The converter itself is composed of the inductor L_s , the capacitor C_{bus} , MOSFET M1 and M2; and Diodes D1 and D2. Buck operation consists of transferring energy from the battery pack to the V_{battery} by triggering MOSFET M2. Boost operation results from triggering MOSFET M1, in this way energy is transferred from the V_{battery} to the V_{dc} . However, on either case the amount of current transferred, if any at all, will depend on the

V_{battery} actual voltage, the system parameters (resistance values, battery voltage) and the duty cycle of the PWM applied. While the energy-transfer's efficiency will depend on these conditions and on the semiconductor's losses. Equations governing the converter will be discussed further on.

In the steady state and for mean values during periods of several seconds, the converter can be modeled as an ideal DC transformer as follows.

For the Boost operation, steady state voltages and currents are described by equations (2-4) and (2-5), respectively. For simplicity, these equations do not take into account the diode's and MOSFET's voltage drop effect. [Micah Ortuzar et al 2003]

$$V_{\text{dc}} = \frac{V_2}{(1-D)} \quad (2-4)$$

$$I_b \approx \begin{cases} \frac{\left(\frac{V_2}{(1-D)} - V_{\text{dc}} \right)}{\left(\frac{R_{\text{int}} + R_2}{(1-D)^2} \right)} & \text{at } \frac{V_2}{(1-D)} - V_{\text{dc}} \geq 0 \\ 0 & \text{at } \frac{V_2}{(1-D)} - V_{\text{dc}} < 0 \end{cases} \quad (2-5)$$

In equations (2-4) and (2-5) R_{int} for the battery's internal resistance, R_2 for the sum of the inductor's resistance and the V_{battery} ESR (Equivalent

Series Resistance); and D stands for the duty cycle of the PWM applied. As it can be seen eq. (2-4) and (2-5), Boost operation can be modeled as a one-way-conducting DC transformer, where the transformer ratio seen from the V_{battery} side is $1/(1-D)$.

Equations (2-6) and (2-7) describe steady state voltages and current during Buck operation. [Micah Ortuzar et al 2003]

$$V_2 = D \cdot V_{\text{dc}} \quad (2-6)$$

$$I_b = \begin{cases} -\frac{(V_{\text{dc}} \cdot D - V_2)}{(R_2 + R_{\text{int}} \cdot D^2)} & \text{at } (V_{\text{dc}} \cdot D - V_2) \geq 0 \\ 0 & \text{at } (V_{\text{dc}} \cdot D - V_2) < 0 \end{cases} \quad (2-7)$$

As in the previous case, Buck operation may be modeled as a one-way-conducting DC transformer, where the transformer ratio seen from V_{dc} is D .

Equations (2-5) and (2-7) do not take into account the ripple component of current. Equations (2-4) through (2-7) will help to understand the converter's behaviour under different conditions and will help to elaborate control strategy. [Micah Ortuzar et al 2003]

2.4.3 Selection of Inductance

In order to produce a controlled DC current through the V_{battery} , small ripple content is desirable. High ripple amplitude also produces other undesired effects, such as losses due to currents induced in other elements; and electromagnetic noise. Therefore, it is desirable to reduce ripple amplitude as much as possible.

Figure (2-3) shows a typical steady state current waveform for a Buck operation.

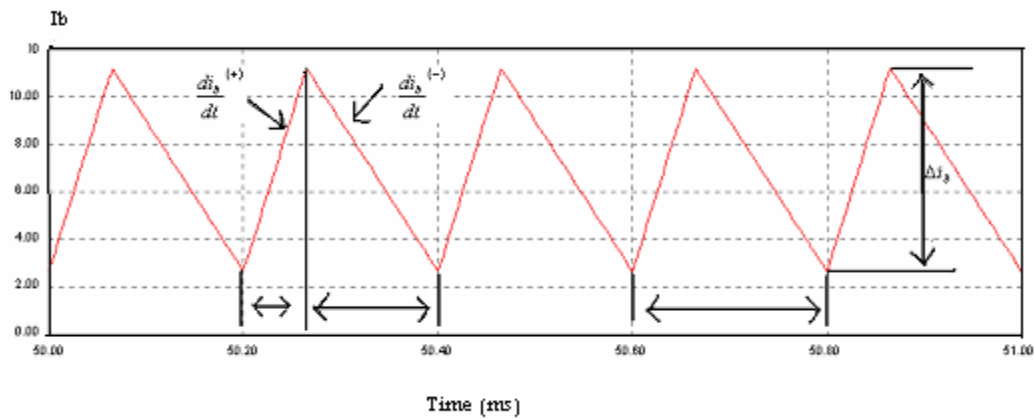


Figure (2-3) Current through V_{battery} ripple waveform

[Micah Ortuzar et al 2003]

Equations (2-8), (2-9) and (2-10) describe the relation between current's components signaled in figure (2-3), which corresponds to current through V_{battery} during a Buck operation. [Micah Ortuzar et al 2003]

$$\frac{di_b^{(+)}}{dt} = \frac{V_{dc} - V_2}{L_s} = \frac{\Delta i_b}{t_o} \quad (R_2 \approx 0, R_{int} \approx 0) \quad (2-8)$$

$$\frac{di_b^{(-)}}{dt} = -\frac{V_2}{L_s} = -\frac{\Delta i_b}{T - t_o} \quad (R_2 \approx 0) \quad (2-9)$$

$$\Delta i_b = \frac{V_{dc}}{L_s \cdot f} \cdot D \cdot (1 - D) \quad \left(f = \frac{1}{T}\right) \quad (2-10)$$

For simplicity, these equations do not take into account the effect of diode and MOSFT voltage drop, nor the voltage drop thorough R_2 and R_{int} resistances.

Deriving with respect to D and zeroing equation (2-10) leads to the value of D for which the ripple amplitude (represented by Δi_b) is maximum. This value is 0.4. Then the maximum value of Δi_b is described by eq. (2-11). [**Micah Ortuzar et al 2003**]

$$\Delta i_b \max = \frac{V_{dc}}{4 \cdot f \cdot L_s} \quad (2-11)$$

Chapter
Three



Design, Modeling and
Simulation

Chapter Three

Design, Modeling and Simulation

3-1 Introduction

This chapter discusses the simulated and design of the battery model. The simulated is carried out using PSPICE software for the complete model in order to get the results for the proposed battery model. Details are also given to the method of measuring the charge efficiency.

3-2 Lead-Acid Battery PSPICE Model

The PSPICE Lead-acid battery model is based on the SPICE, which consists of the charge efficiency and battery voltage components. The charge efficiency component was originally developed at Lockheed Martin/Sunnyvale. The schematic of the Pspice model is shown in figure (3-1). The voltage component of the model consists of amp-hour integrator which tracks the net current flowing into the battery terminal (V_{battery}). The output of the integrator give us the SOC according to eq (3-1) so, it is connected to a table driven voltage source, ETABLE, which generates the equivalent open circuit battery voltage (V_{battery}) according to the piecewise linear curve shown in appendix(A). [Greg Waldo 2002]

$$SOC = \frac{1}{RC} \int V_{in} dt \quad (3-1)$$

As the battery is charged, less and less charge current contributes to an increase (SOC) instead being converted to heat. The model accounts for the changing battery efficiency by multiplying the battery current by a factor called charge efficiency.

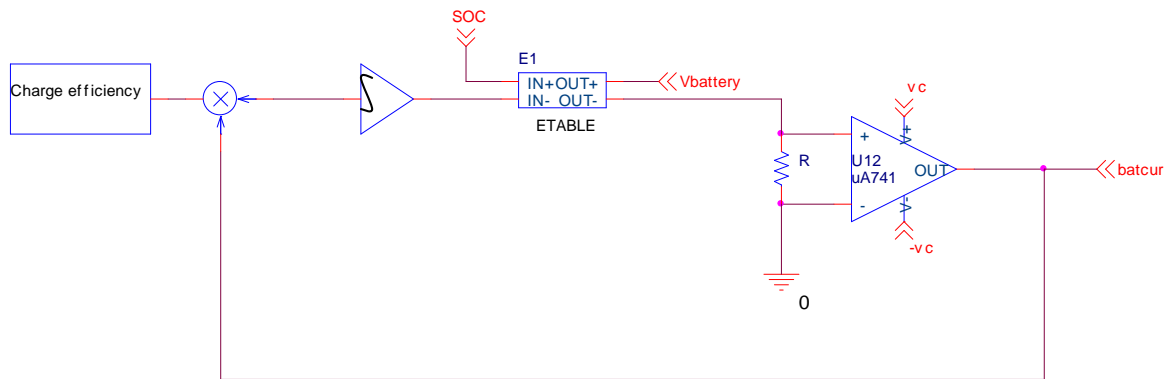


Figure (3-1) Pspice lead-acid battery model

3.2.1 Charge Efficiency Factor

Charge efficiency factor can vary from 0 to 1 and is dependent on the battery SOC, charge current and temperature. If battery SOC is negative, or battery is in discharge, then charge efficiency equal one, otherwise it becomes as in eq.(3-2) [Greg Waldo 2002]

$$\text{Charge efficiency} = \frac{1}{1+r} \quad (3-2)$$

where

$$r = \exp \left(\frac{-r_t}{e_2} \right) \quad (3-3)$$

and

$$r_t = \text{eterm1} + \text{eterm2} + \text{eterm3} \quad (3-4)$$

These terms (term1, term2, term3) represents the three parameters affected in a charge efficiency factor. [Greg Waldo 2002]

$$eterm1 = a1 * \log (e1 * batcur) \quad (3-5)$$

$$eterm2 = -a2 * \log \left[\frac{SOC}{(KEBatcap * batcap - SOC)} \right] \quad (3-6)$$

$$eterm3 = a3 * (25 - tempC) + a4 \quad (3-7)$$

where

a1, a2, a3, a4, e1 and e2 are constants and their values are explained in table (3-1) and

KEBatcap = Battery theoretical capacity/nameplate capacity

Batcap = capacity (A.h)*K sec per (hr)

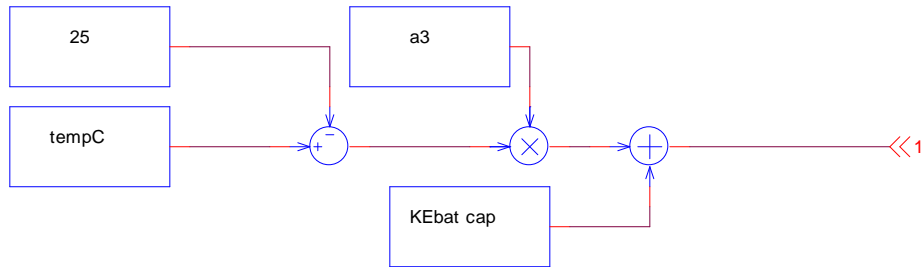
Ksecper(hr) = second/hour = 3600

Table (3-1) Parameters of used in equations for Lead acid battery

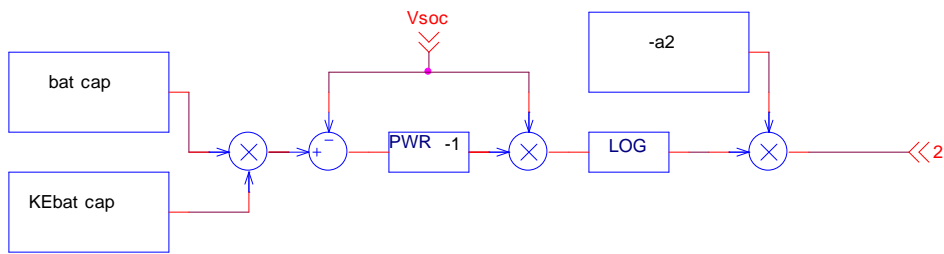
[Greg Waldo 2002]

Parameters	Value
a1	0.009
a2	-0.028
a3	2.677e-4
a4	0.10566
e1	-0.0055*KSecperHr/(KEBatCap*batcap)
e2	0.005
KEBatCap	0.84
TempC	50
KSecPerHr	3600
batcap	288000

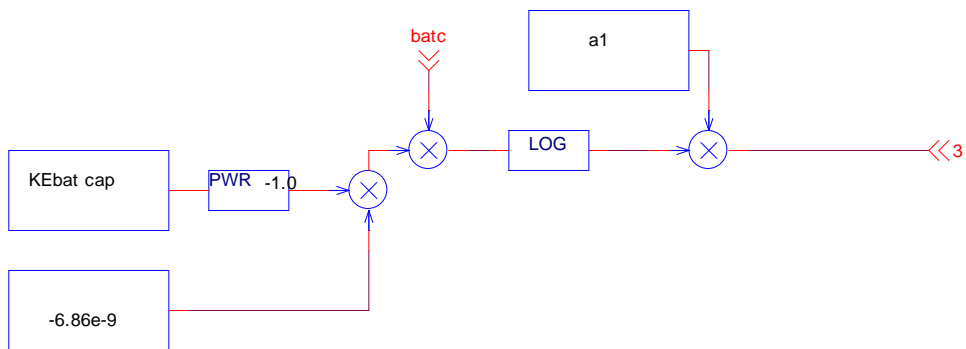
The Analog Behavioral Modeling (ABM) is used to define these three terms as shown in figure (3-2). Figure (3-3) shows the complete circuit of the charge efficiency factor as represented by ABM in PSPICE.



(a)



(b)



(c)

Figure (3-2) r_t three terms as represented by ABM in PSPICE

- (a) **eterm1**
- (b) **eterm2**
- (c) **eterm3**

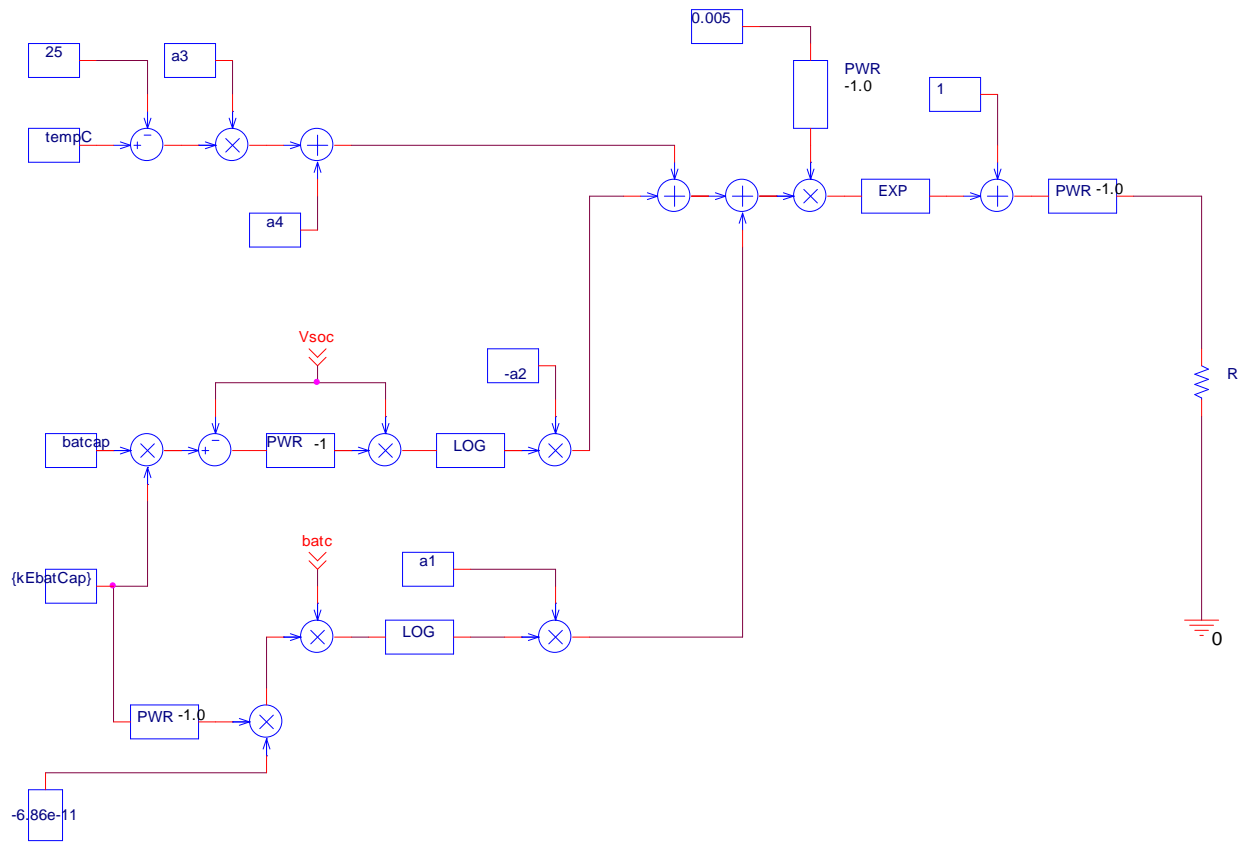


Figure (3-3) the charge efficiency factor as represented in PSPICE

3.2.2 Battery Voltage Components

The voltage component of the battery PSPICE model is shown in figure (3-4). The output of the charge efficiency factor is applied to the integrator OP1 (uA741) after multiplying it by the battery current ($bat\ cur$) (the output of OP2) in order to change the battery efficiency. The nominal battery resistance (R_{batt}) is connected between the two terminals of (OP2). The output of the integrator is applied to the ABM part (gain of 5) for expanding the range of SOC to 75.

The Etable part (E1) is used to generate the battery voltage. This part use a transfer function described by a table. The table consists of the pairs of values, the first of which is an input, and the second of which is the corresponding output. Linear interpolation is performed between entries. For

values of outside the table's range, the devices output is a constant with a value equal to the entry with the smallest (or largest) input. The characteristic can be used to impose an upper and lower limit on the output. [Greg Waldo 2002]

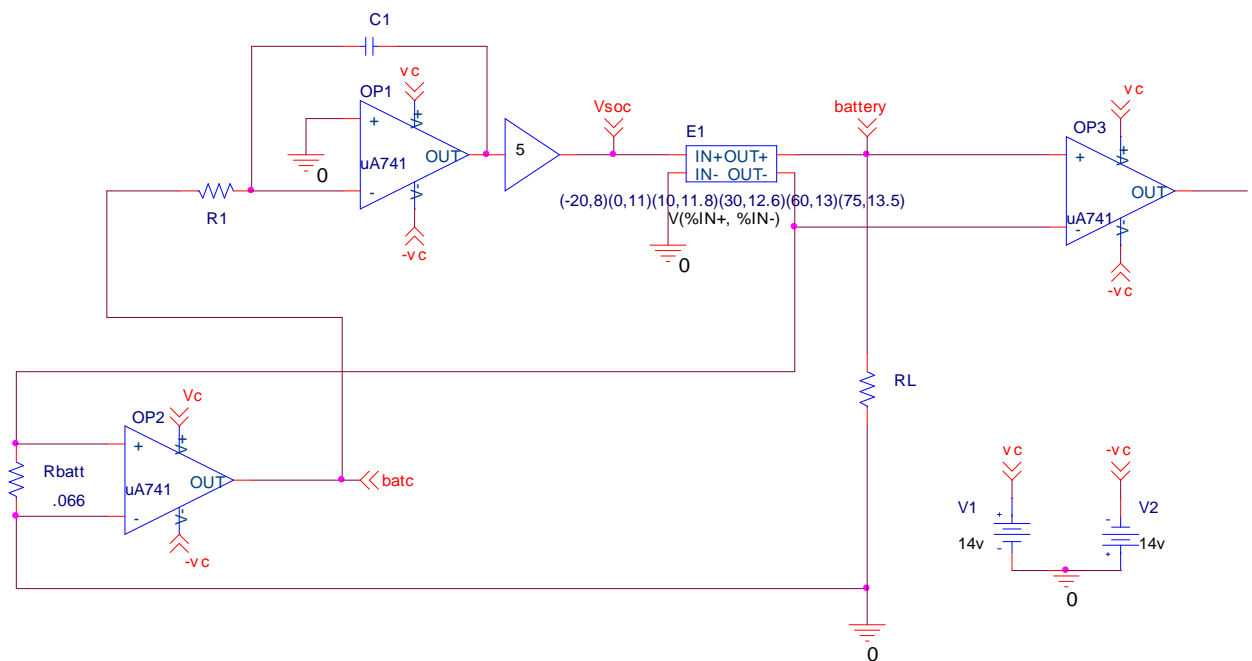


Figure (3-4) the battery voltage component represented in PSPICE

The model described in the previous paragraph has been implemented in the orcad-pspice. The complete model shown in figure (3-5) has been verified and used to find the optimal operation.

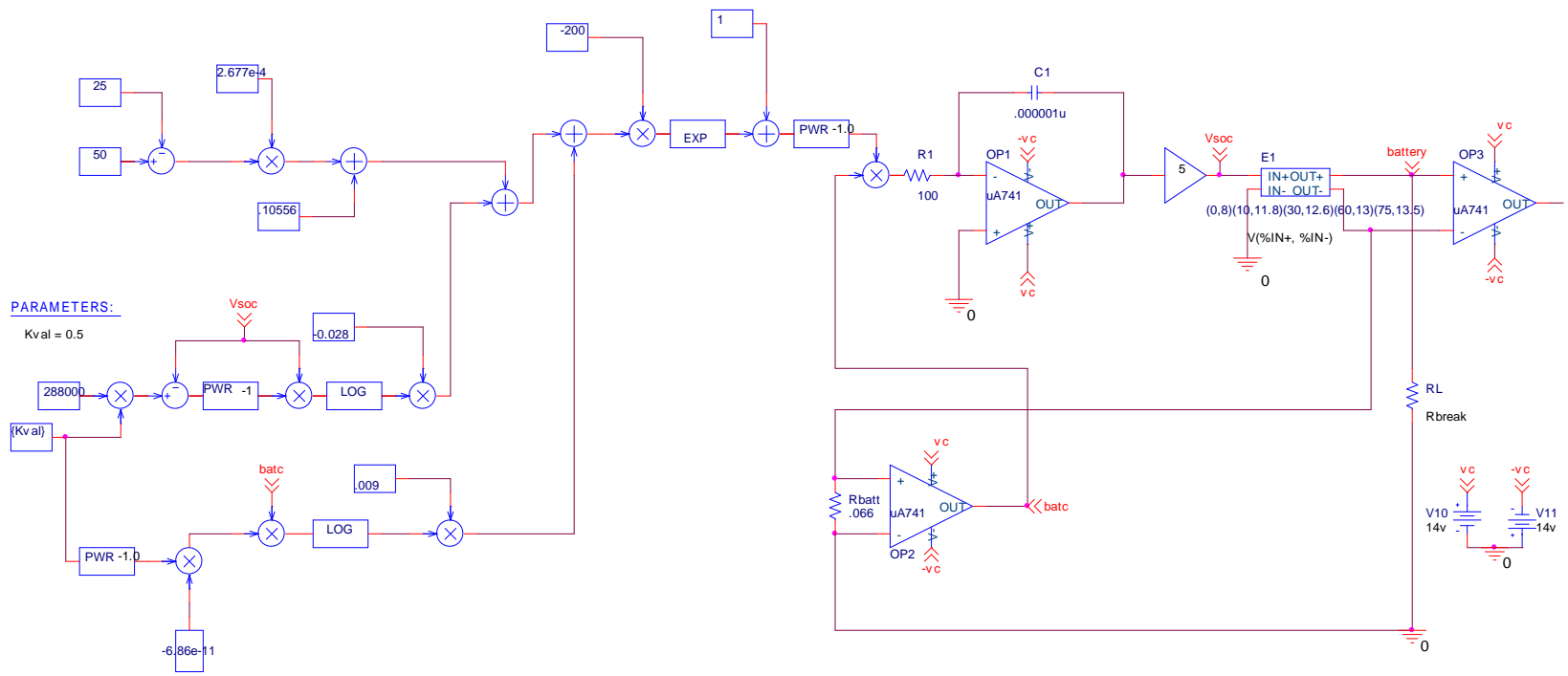


Figure (3-5) complete circuit of the battery as represented in PSPICE.

3.3 Converter Circuit Design

In continuous condition mode, the bidirectional boost converter that to be designed is for output voltage 12V, switching frequency 1 kHz, duty cycle 0.4 and power 12W. Figure (3-6) shows the non isolated single-phase bidirectional boost as represented in PSPICE. This converter is consist of two MOSFT (IRF460), inductor (L1), capacitors (C_{batt} , C_{bus}) and resistance (R_2). The connection of blocking diode after the MOSFT is necessary to prevent any leakage current passing through the MOSFT that might interfere with the operation of the converter.

As it was mentioned before, the battery pack's nominal voltage (V_{dc}) is 12V. The frequency of 1 kHz has been arbitrarily chosen in order to minimize current ripple, while maintaining low commutation loses and operating the MOSFT within its recommended range.

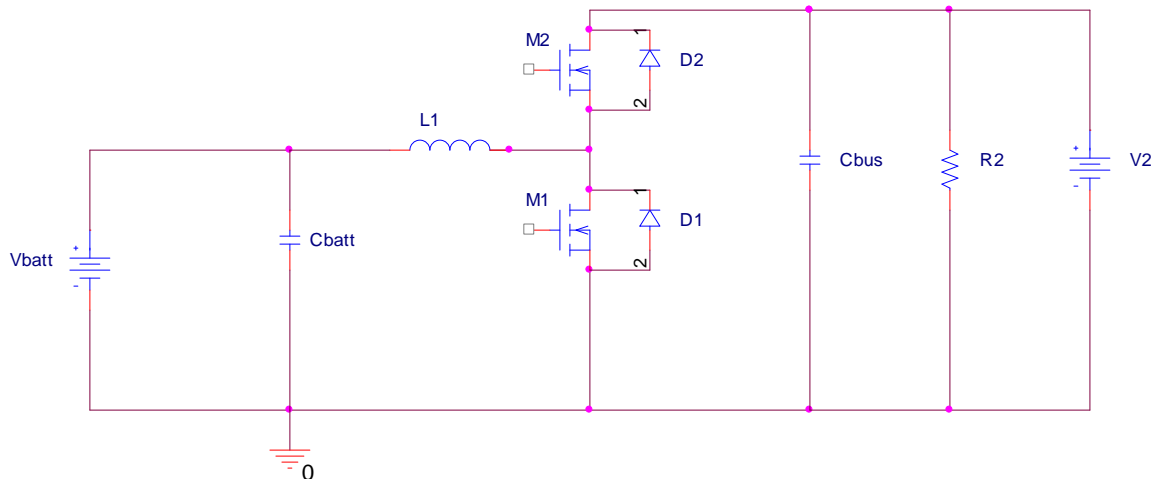


Figure (3-6) Non-Isolated Single-Phase Bidirectional Buck Boost converter

Power flows from the auxiliary power unit to the DC bus when Q2 and M1 are active (Q1 and M2 are inactive) while the power flows from the DC bus when the pack Q1 and M2 are active (Q2 and M1 are inactive).

A ripple of 0.6A was established as the maximum desired value. Therefore, the inductance value L1 is calculated according to eq. (2-12) (6mH), C_{bus} (20.8μf) and C_{batt} (10.4μf).

3.4 Pulse Width Modulation (PWM) and Gate Drive Circuit

This unit generates the signal with necessary duty ratio to drive the switching devices of the converter as shown in figure (3-7).

The error amplifier U3 (uA741) detects the error output result from the difference between the reference voltage (V1) and the actual voltage (battery). This error level is applied to the comparator U4 (uA741) which compare with the saw tooth signal that properties (V_{peak} =15V, T_{period} = 2ms). The output of the PWM generator is connected to the buffer circuit U9 (uA741) in order to isolate the output PWM from transistor Q1. The transistor Q1 operates as (not gate) and figures as MOSFT gate drive circuit through a resistance R4.

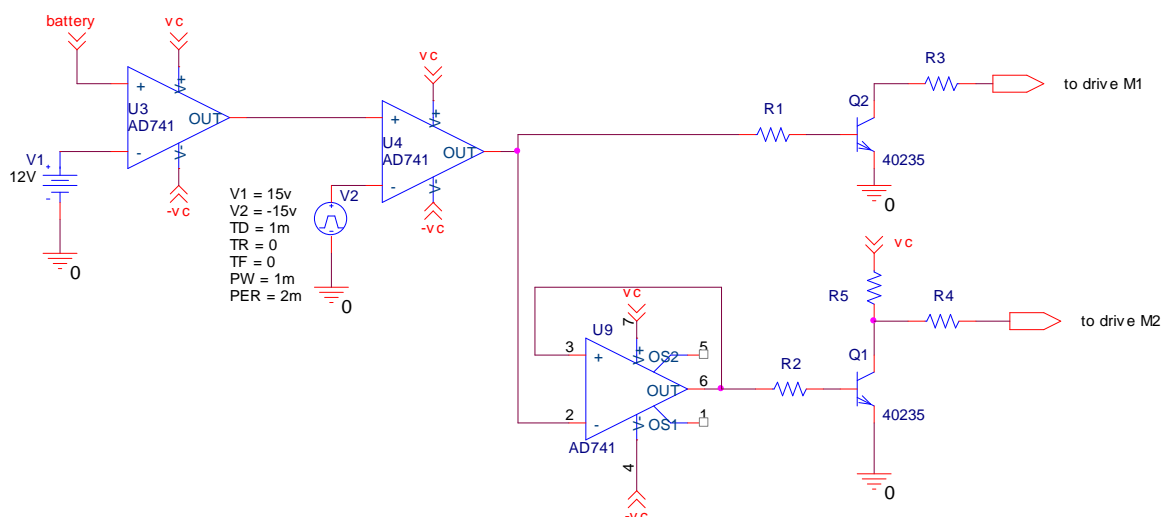


Figure (3-7) the system of the PWM generator and gate drive circuit

3.5 Boot-Strap Circuit Technique (BSCT)

The Boot-Strap circuit, which uses diode and capacitor, is shown in figure (3-8). When the low side power switching device is turned on, the floating supply capacitor is charged through the Boot-Strap diode. When the low side of the switching device is off, the energy stored in the capacitor provides power for the high side gate drive. The Boot-Strap circuit is very effective method for providing power for the high side of power switching gate drive. However care must be exercised to maintain the high side supplies when the inverter is idle and during fault handing conditions.

This usually means that the low side of power switching must be pulsed on periodically even when the inverter is not running. At power up, the Boot-Strap supplies must be changed before the PWM is started. [Kubba Z.M 2003]

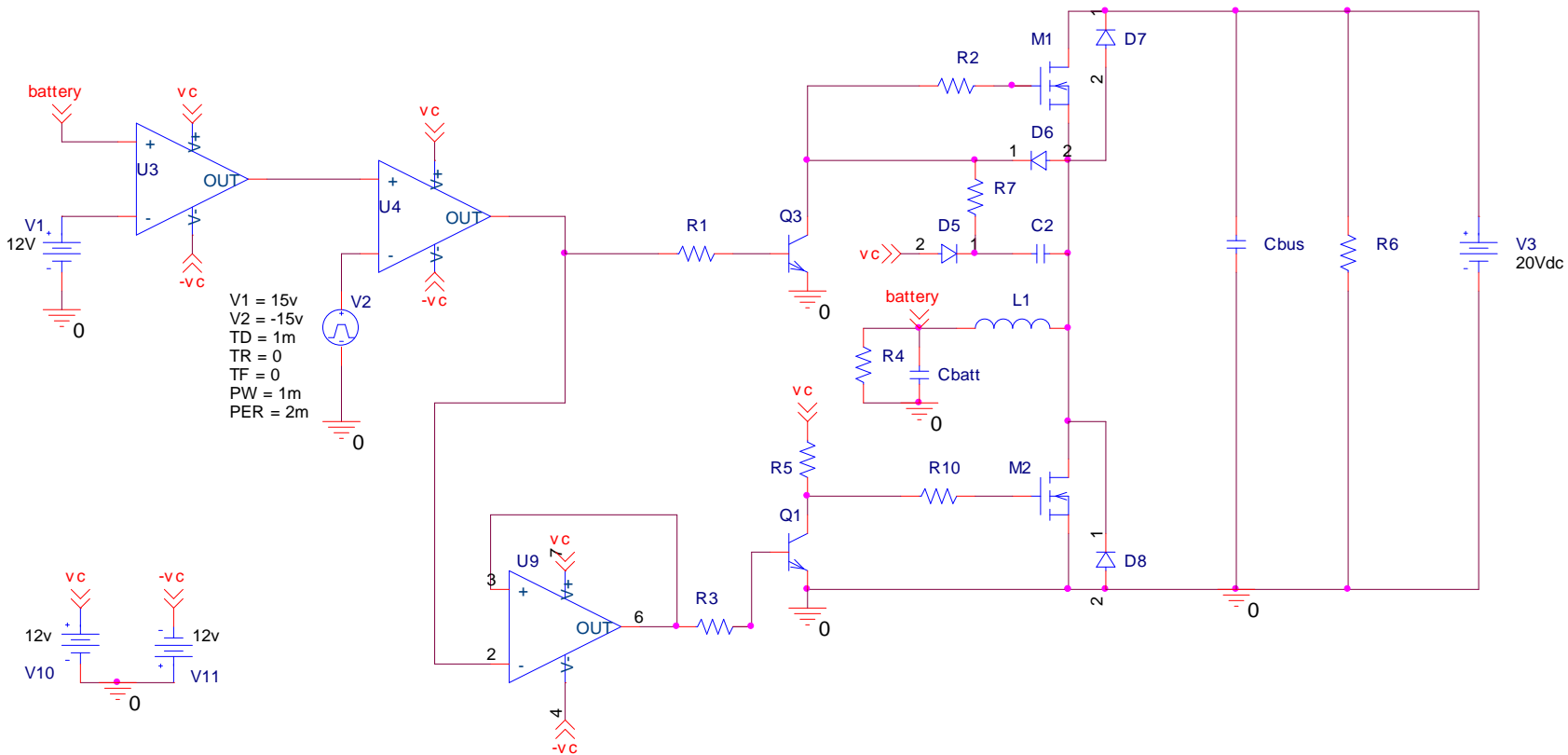


Figure (3-8) complete circuit of the converter as represented in PSPICE.

Chapter
Four

Results & Discussion

Chapter Four

Results and Discussion

4.1 Battery Model Simulation

Three parameters affect the results of this model R_L , R_{batt} and $K_{Ebat\ cap}$. First the model was tested by varying the load, therefore R_L defined as R_{break} , $R_{batt}=0.066\Omega$ and $K_{Ebatcap}=0.88$. From the transient analysis figure (4-1) shows the battery voltage for three cases (0.1 Ω , 0.3 Ω , 0.5 Ω), the one that shows the highest $V_{battery}$ belongs to the lowest R_L (0.1 Ω), and so on. The figure also shows that all the curves starts for (8V) and increases up to the region of the steady state at (90ms). The curves for (0.3 and 0.5) shows very close to each other and some time they seem to be coincide. The curve for (0.1 Ω) shows similar behaviour to the (0.3 Ω and 0.5 Ω) but with higher values of $V_{battery}$. A good similarity between this curves but $V_{battery}$ decreases as R_L increased.

Next the following figures (4-2) (4-3) describe the state of charge and charge efficiency for three cases of R_L (0.1 Ω , 0.3 Ω , 0.5 Ω). Figure (4-2) indicates that the SOC increases gradually with charge time all the curves starts for zero and increases up to the region of steady state at (95ms) but charge efficiency decreases gradually with time in figure (4-3) shows the curves of charge efficiency for the (0.1 Ω , 0.3 Ω and 0.5 Ω). It is very clear that the charge efficiency is higher for more stable curves (curves of little drop) and those of severe drop are of less charge efficiency. The highest charge efficiency is for the lowest R_L (0.1 Ω) and the lowest charge efficiency is for the highest R_L (0.5 Ω). SOC and charge efficiency are decrease as R_L increase. The battery voltage as a function of the SOC is described in figure (4-4) for $R_L=0.5\Omega$, it reveals that the battery voltage increased linearly with the SOC increased according to eq (2-2). Figure (4-5) shows a plot of charge efficiency

as a function of the SOC and it shows that the first drops severely as the SOC increase for $R_L=0.5\Omega$, $R_{batt}=0.066\Omega$.

Now, the model will be tested by varying $K_{Ebatcap}$ so, this factor defines as K_{val} (varying parameter), $R_{batt}=0.066\Omega$ and $R_L=0.7\Omega$. The same figures which explained in the first test are repeated here in figures [(4-6), (4-7), (4-8), (4-9) and (4-10)]. These figures differ from the first test that the battery voltage, SOC and charge efficiency increases as the $K_{Ebatcap}$ increased. Also in figure (4-8) the charge efficiency of smallest value of $K_{Ebatcap}$ reaches (0.25) faster than the biggest value.

The last test is determined by defining R_{batt} as K_{val} while the other factor is constant ($R_L=0.7\Omega$, $K_{Ebatcap}=0.3$). The battery voltage is affected by R_{batt} value as shown in figure (4-11) three curves for three R_{batt} (0.066 Ω , 0.086 Ω and 0.106 Ω) these curves shows very close to each other and some time they seem to be coincide. All curves starts for (8V) and increase up to the region of the steady state of (50ms) but the SOC and charge efficiency gives a little affect as R_{batt} increased as shown in figure (4-12), (4-13) respectively.

The battery parameters (battery voltage, SOC and charge efficiency) is affected by temperature and this effect is explained in figure (4-14), (4-15) and (4-16) respectively. Figure (4-14) shows two curves for the two temperature (30°C and 10°C) starts for (8V) and increases up to the region of the steady state at (76ms). Figure (4-15) shows two curves for the two temperature (30°C and 10°C) starts for (zero) and increases up to the region of the steady state at (85ms). Figure (4-16) shows the curves of charge efficiency for the (30°C and 10°C) the charge efficiency of smallest value reaches (0.1) and two curves starts for (1) and decrease down to the region of the steady state at (80ms).

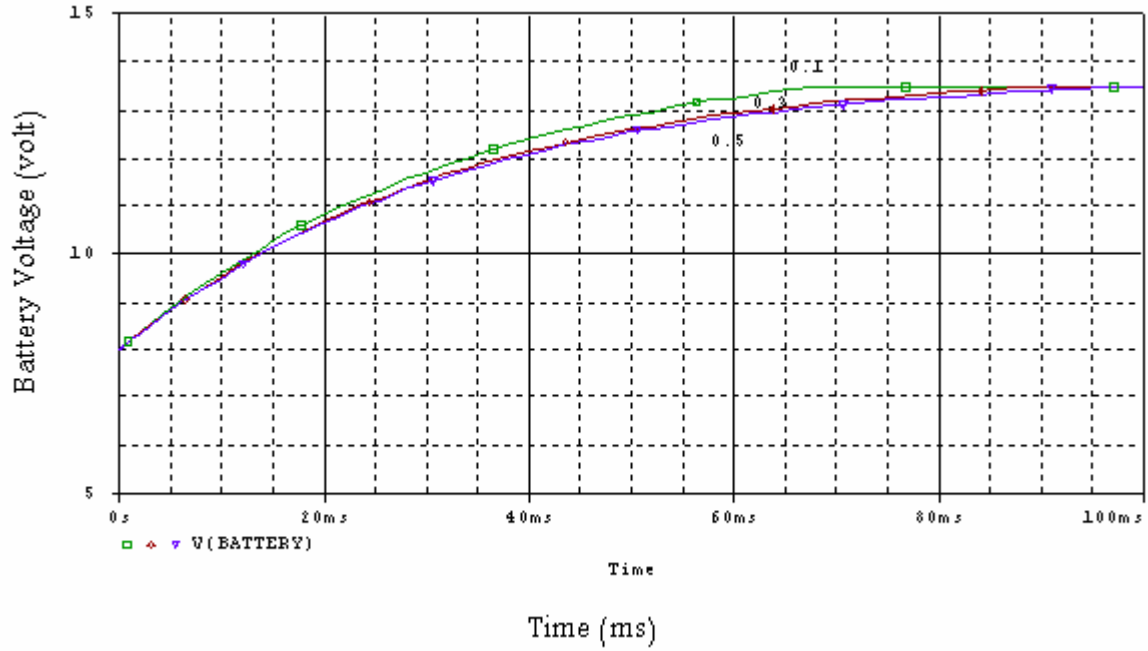


Figure (4-1) battery voltage as a function of time at different RL (0.1Ω , 0.3Ω , and 0.5Ω)

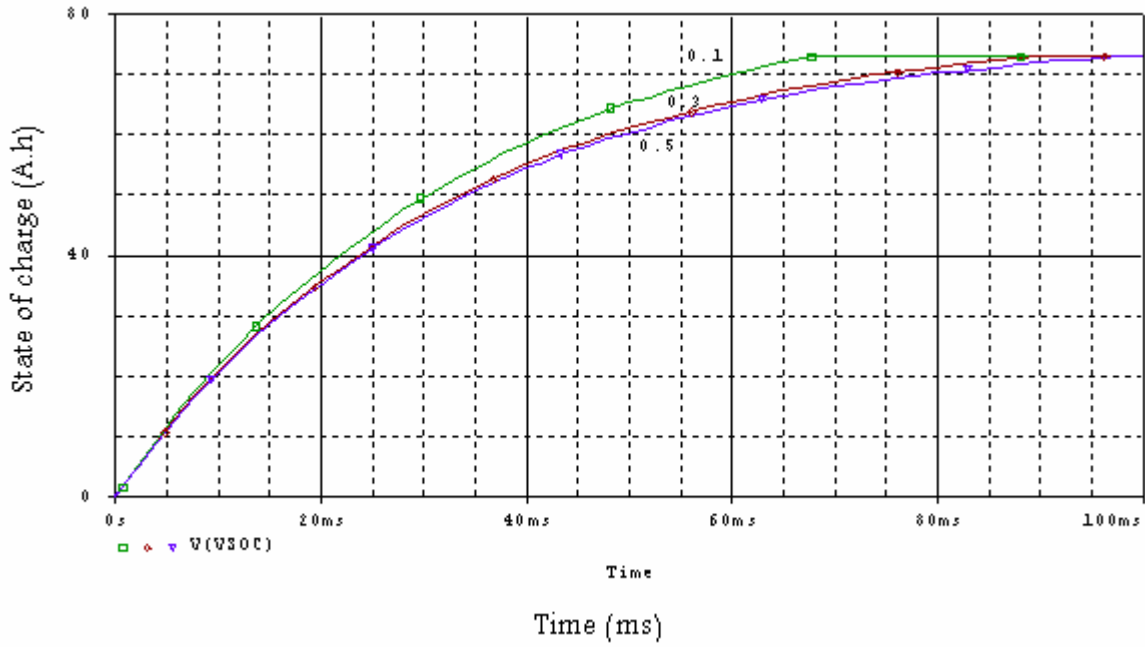


Figure (4-2) state of charge as a function of time at different RL (0.1Ω , 0.3Ω and 0.5Ω)

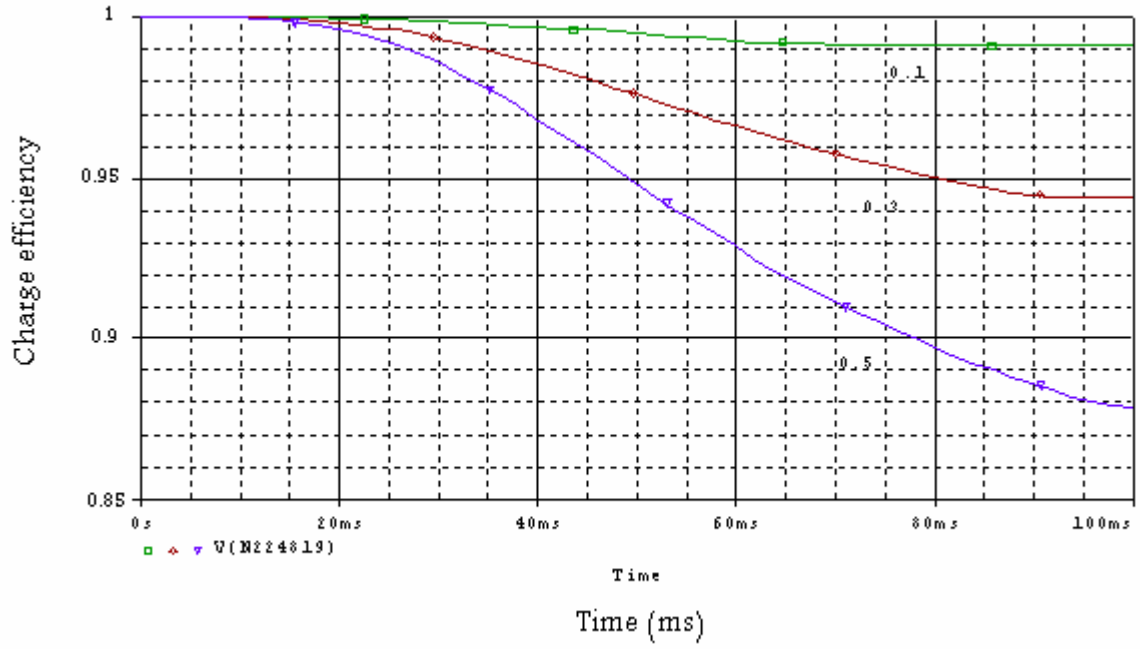


Figure (4-3) charge efficiency as a function of time at different RL (0.1Ω, 0.3Ω and 0.5Ω)

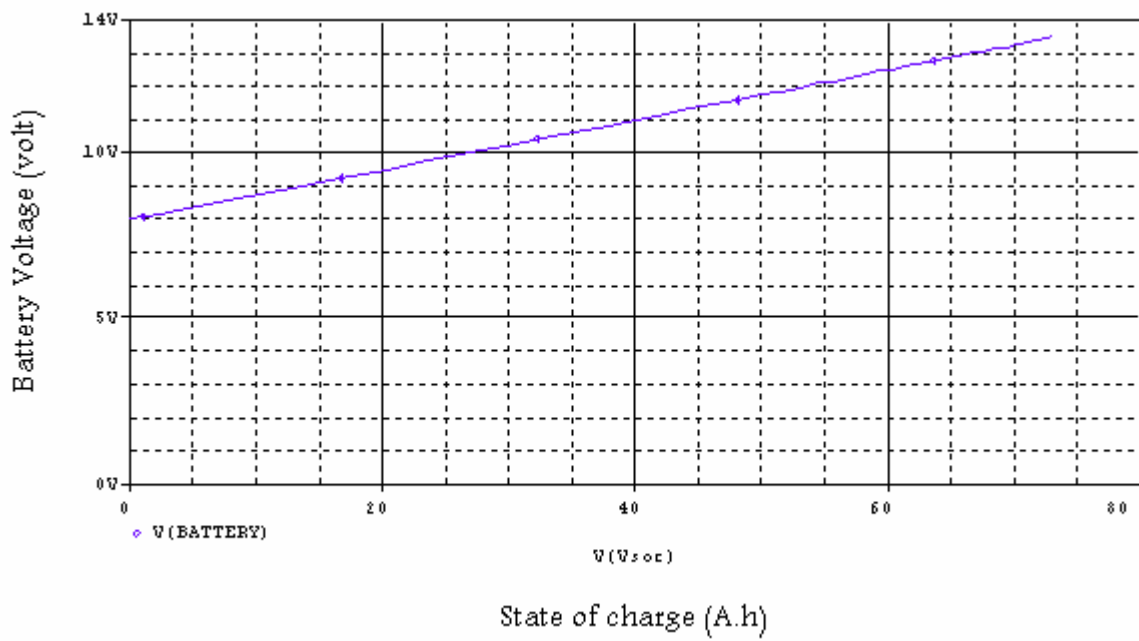


Figure (4-4) battery voltage as a function of state of charge at RL=0.5Ω

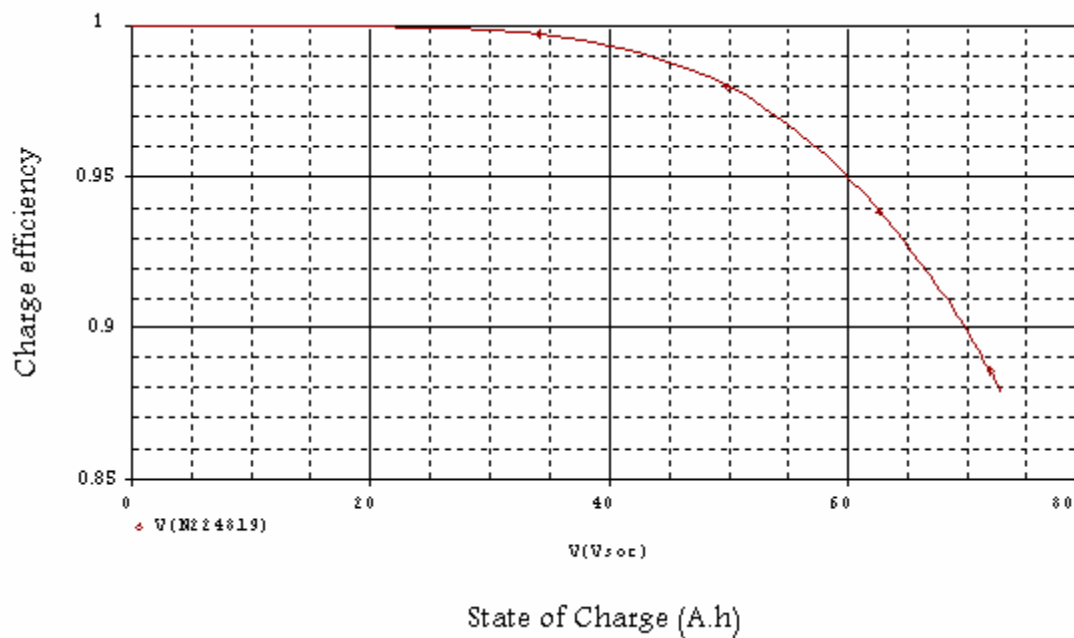


Figure (4-5) charge efficiency as a function of state of charge at $RL=0.5\Omega$

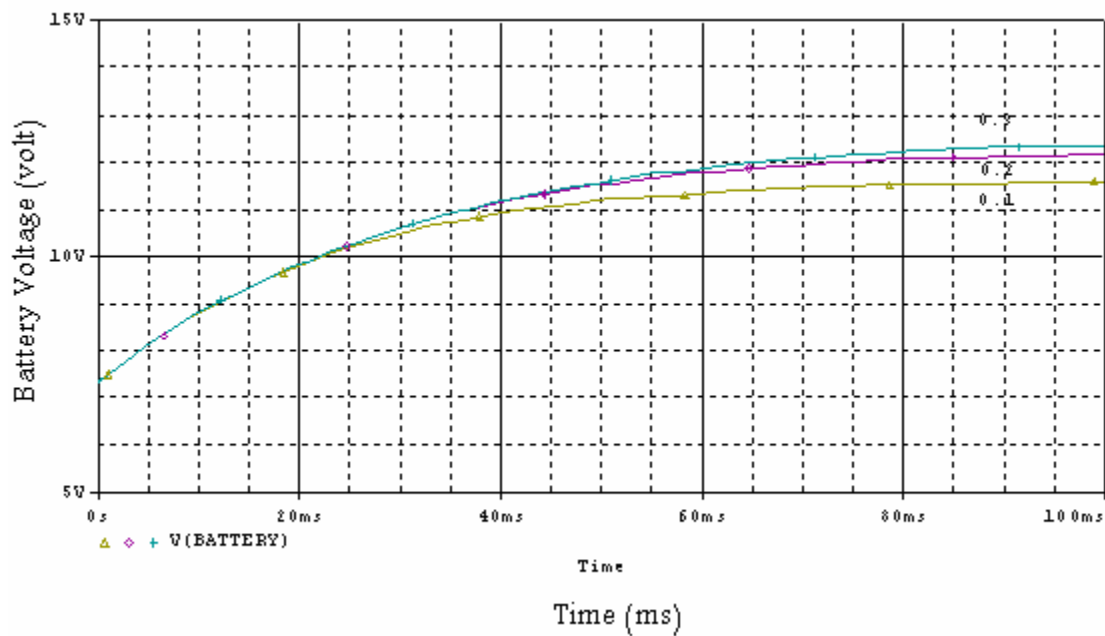


Figure (4-6) battery voltage as a function of time at different Kval (0.1, 0.2 and 0.3)

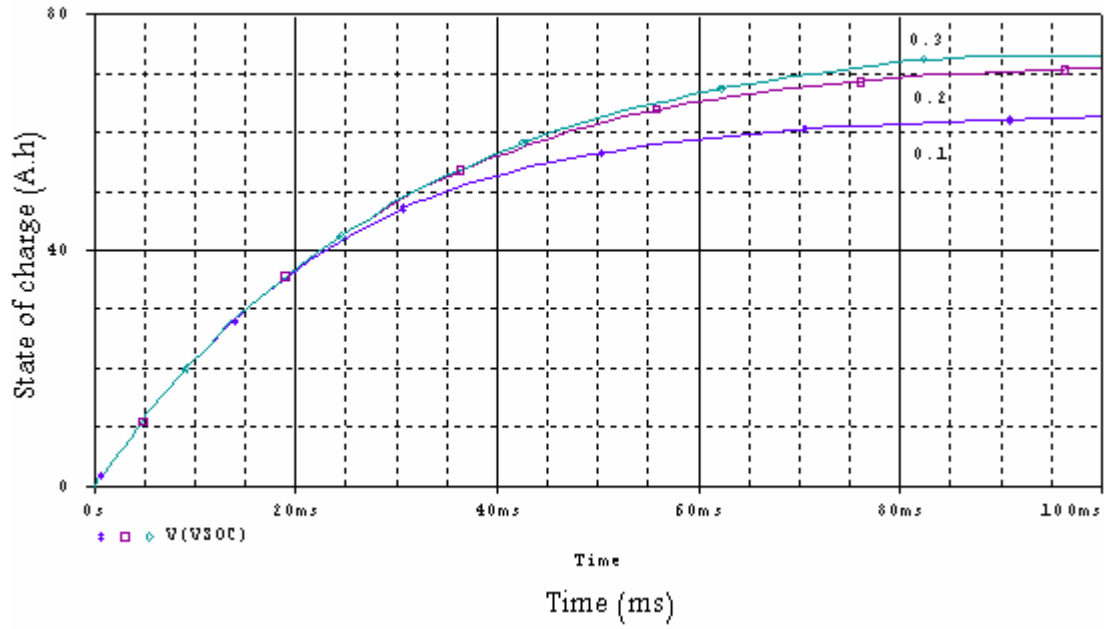


Figure (4-7) state of charge as a function of time at different Kval (0.1, 0.2 and 0.3)

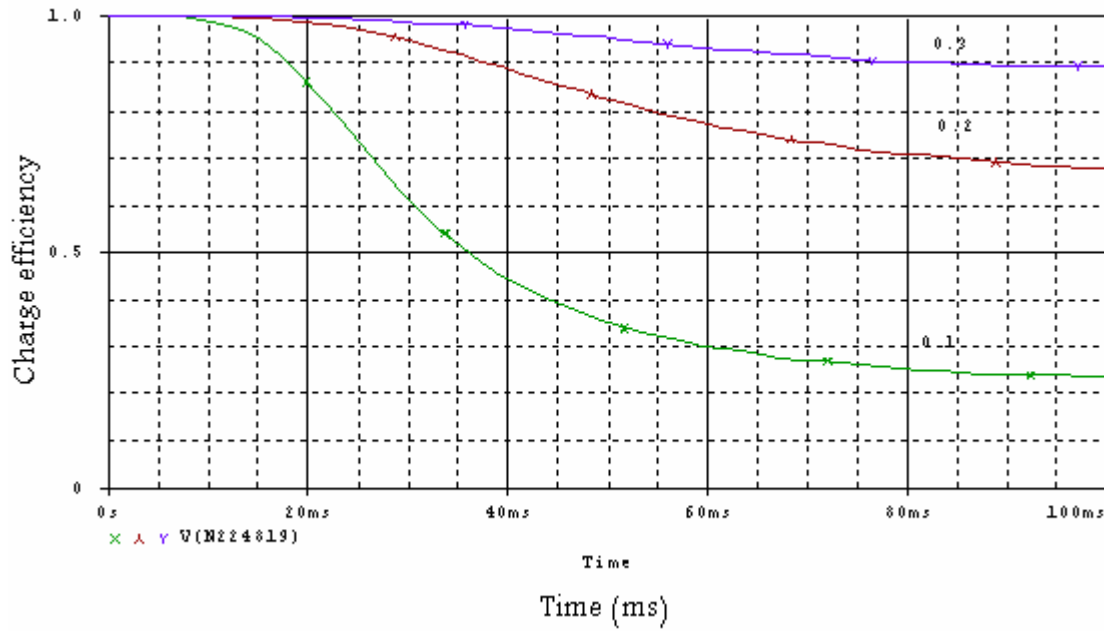


Figure (4-8) charge efficiency as a function of time at different Kval (0.1, 0.2 and 0.3)

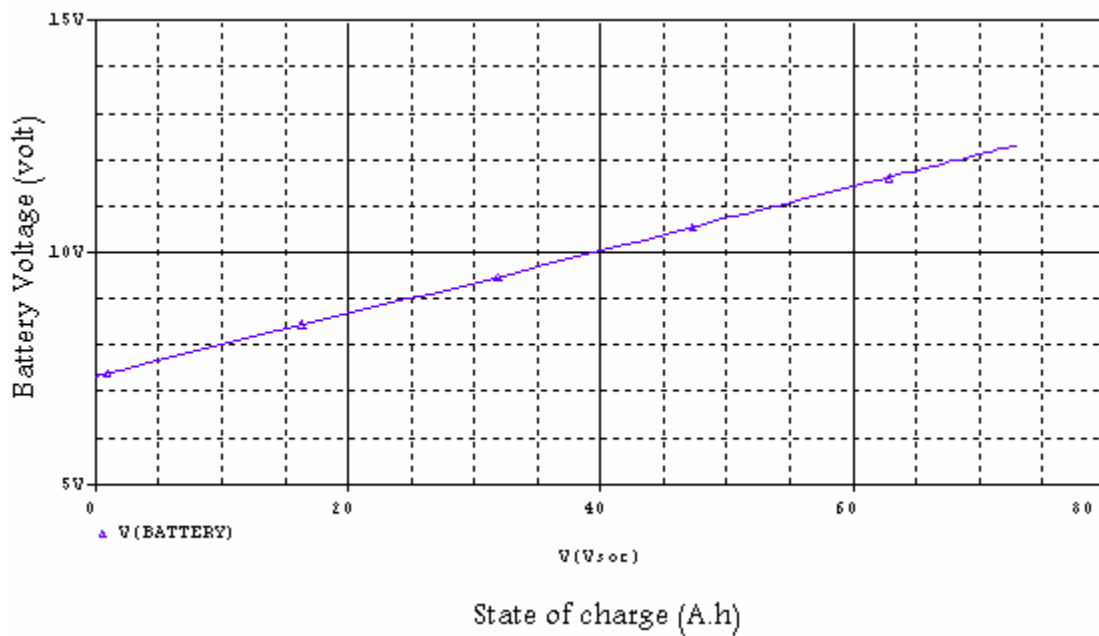


Figure (4-9) battery voltage as a function of state of charge at Kval=0.3

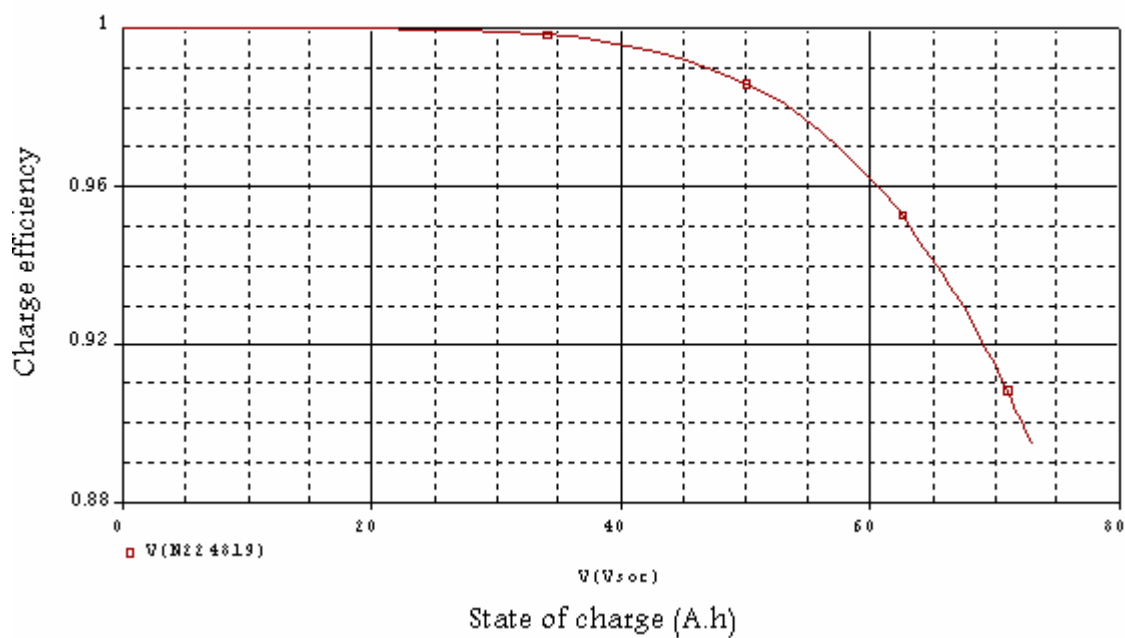


Figure (4-10) charge efficiency as a function of state of charge at Kval=0.3

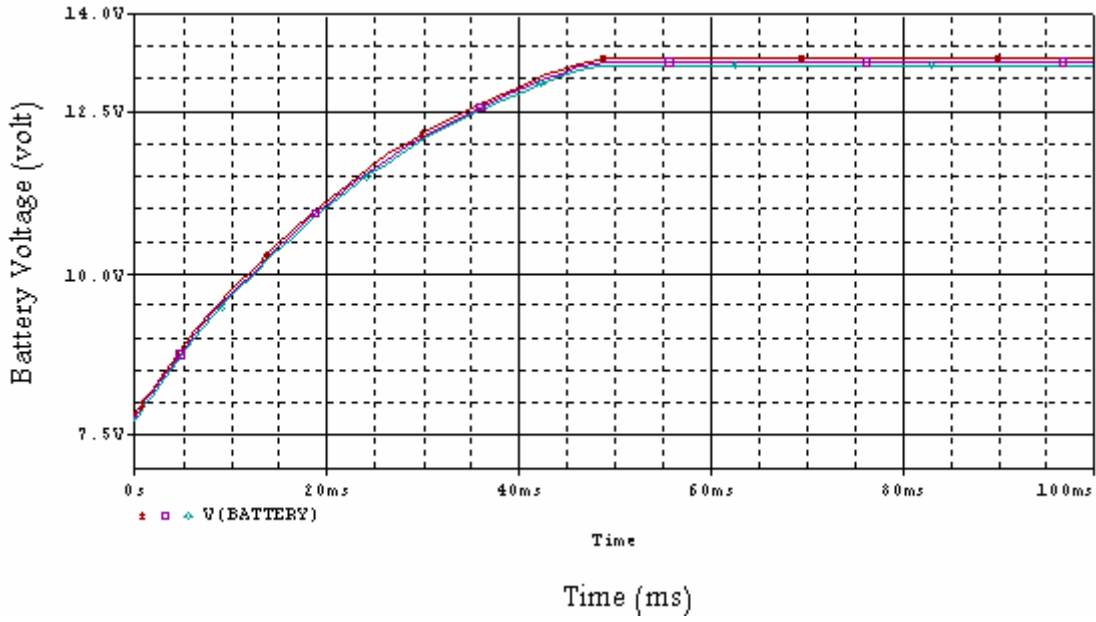


Figure (4-11) battery voltage as a function of time at different R_{batt} (0.066Ω , 0.086Ω and 0.106Ω)

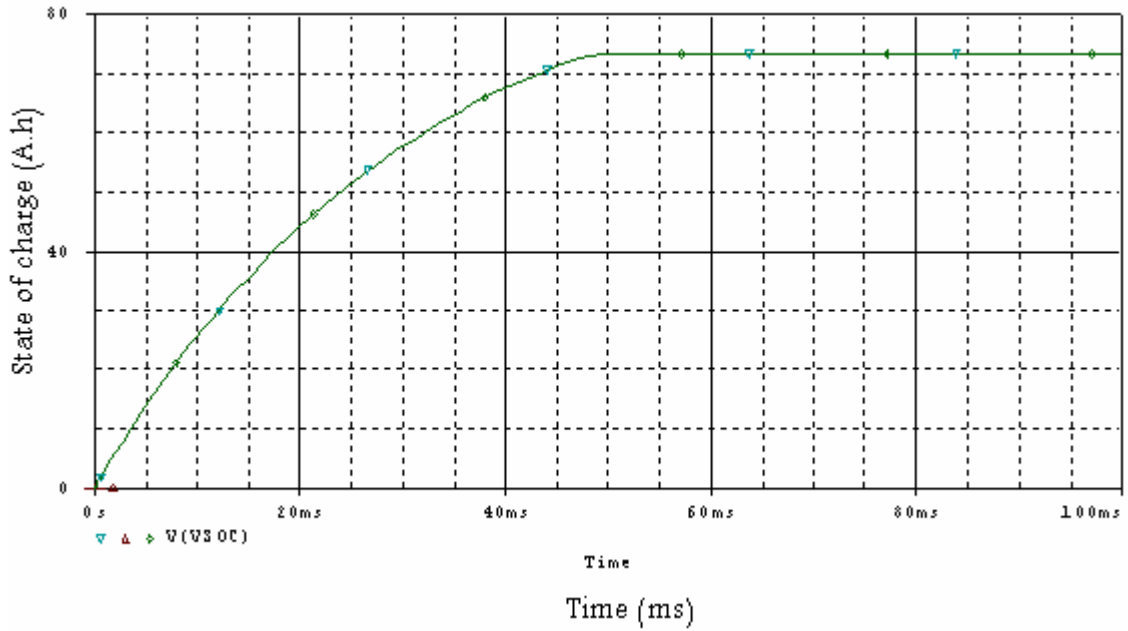


Figure (4-12) state of charge as a function of time at different R_{batt} (0.066Ω , 0.086Ω and 0.106Ω)

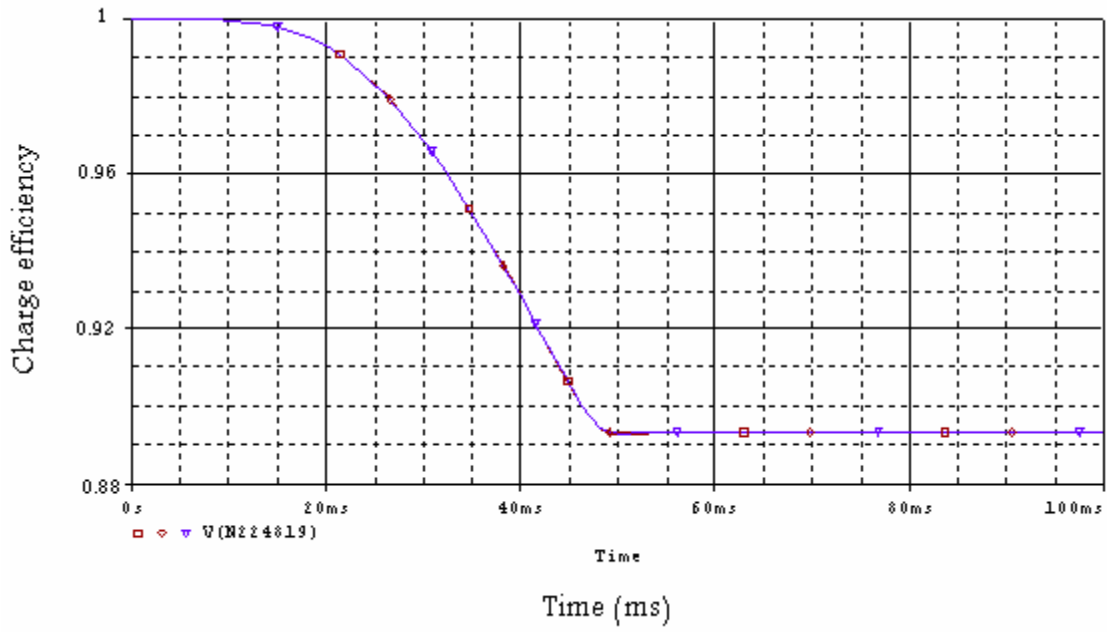


Figure (4-13) charge efficiency as a function of time at different R_{batt} (0.066Ω, 0.086 Ω and 0.106Ω)

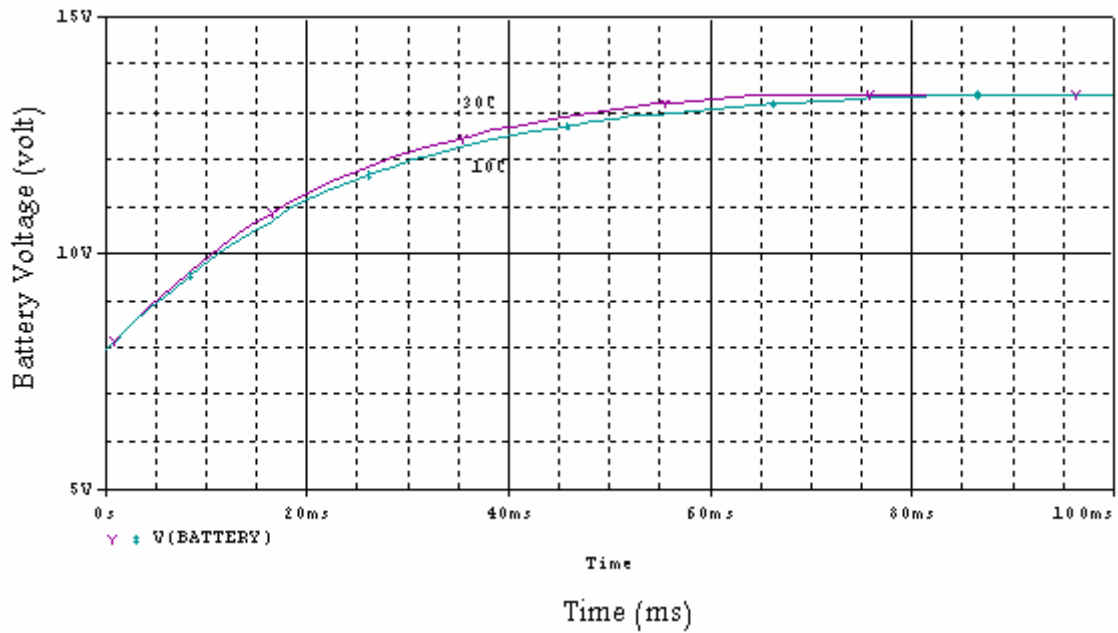


Figure (4-14) battery voltage as a function of time at different temperature

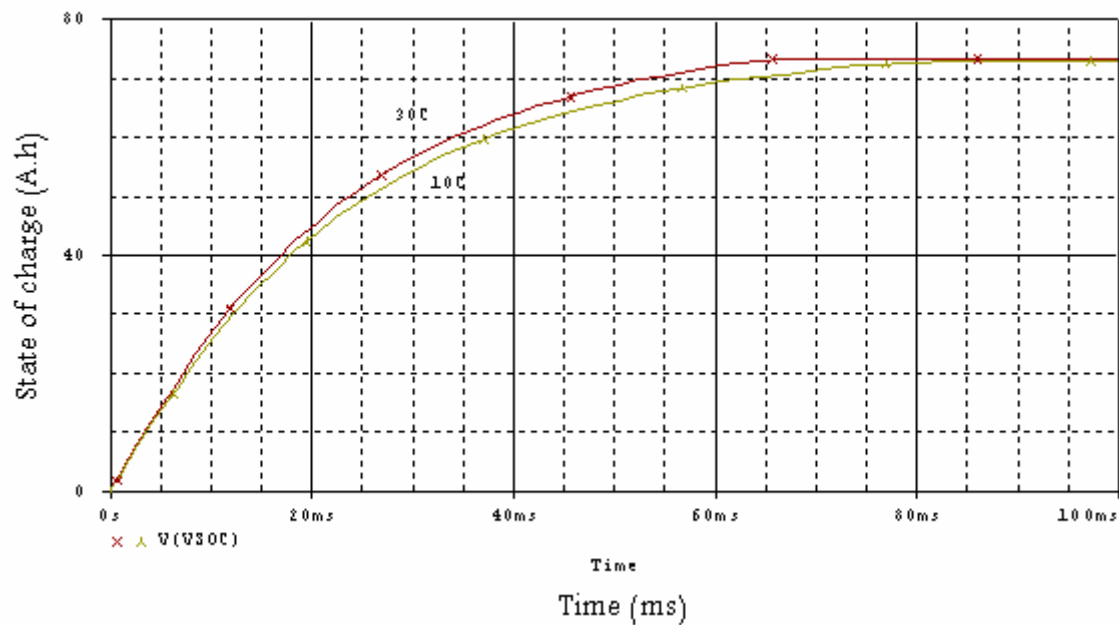


Figure (4-15) state of charge as a function of time at different temperature

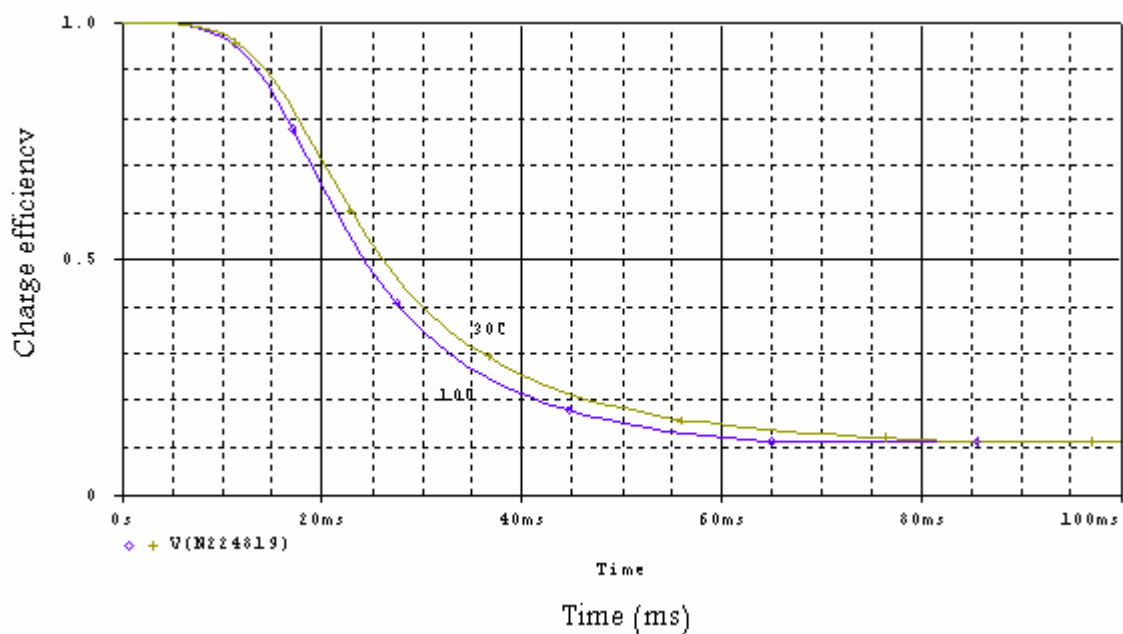


Figure (4-16) charge efficiency as a function of time at different temperature

4.2 Analytical Result obtained by PSPICE

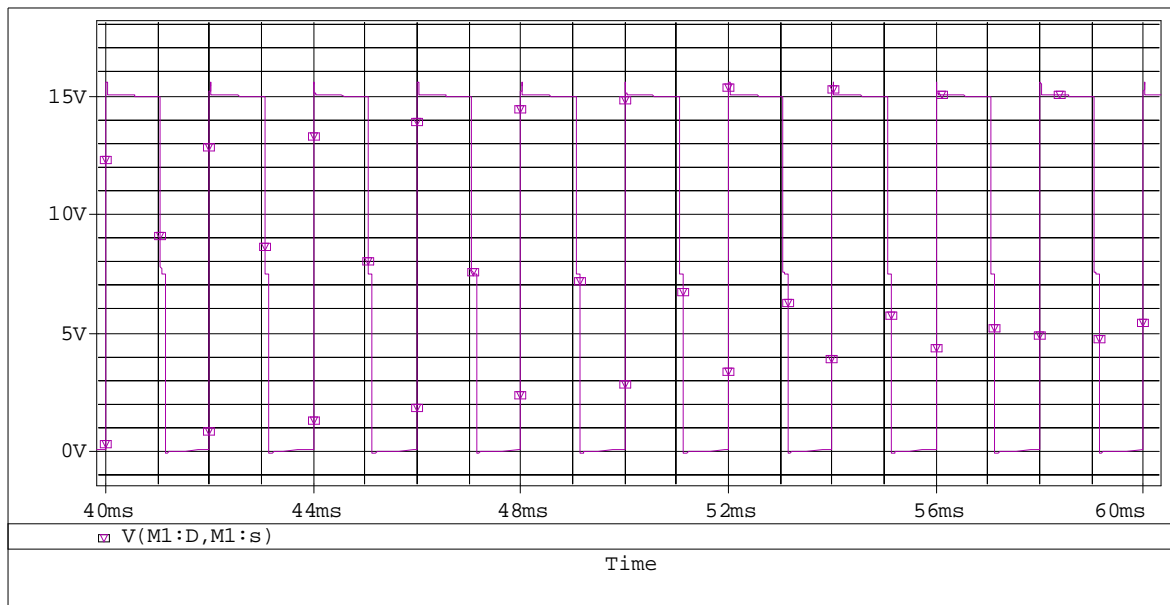
The proposed bidirectional boost converter system is shown in figure (3-8). The analysis of this system was carried out to obtain the waveform and result of each stage by using PSPICE software and comparing these with the predicted results obtained by circuit design to confirm that the chosen model work satisfactory.

The bidirectional boost converter configuration will be discussed as follows:

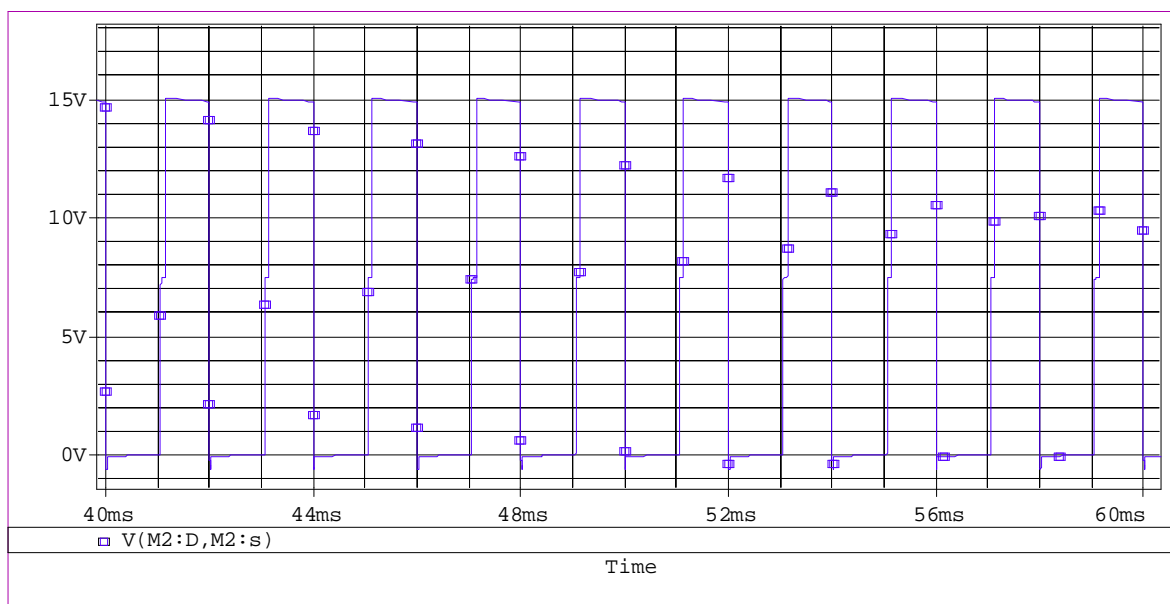
Figure (4-17) shows two voltage responses for drain to source of M1 and M2, one for buck operation and the other for boost operate. The output of two states is out of phase.

Figure (4-18) show the output ripple voltage. The maximum voltage is equal to 10.5V and the minimum voltage is to 4.5V.

As expected the maximum ripple content was produced at duty cycle of 0.4 and its value of less than 1A (about 0.6A) as shown in figure (4-19).



(a)



(b)

Figure (4-17) Voltage of converter

(a) Voltage Across M1

(b) Voltage across M2

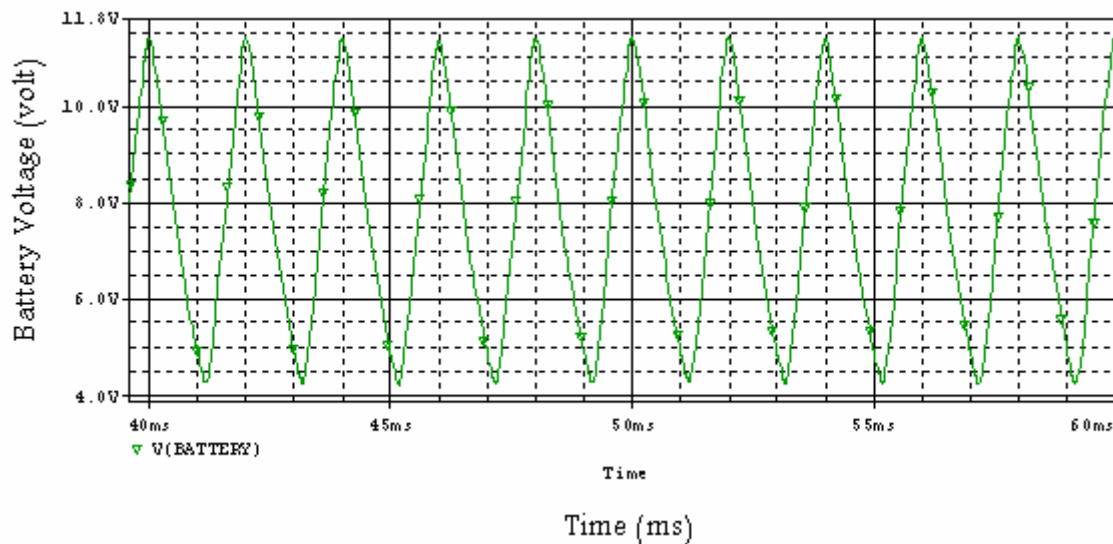


Figure (4-18) Output Voltage of bidirectional converter

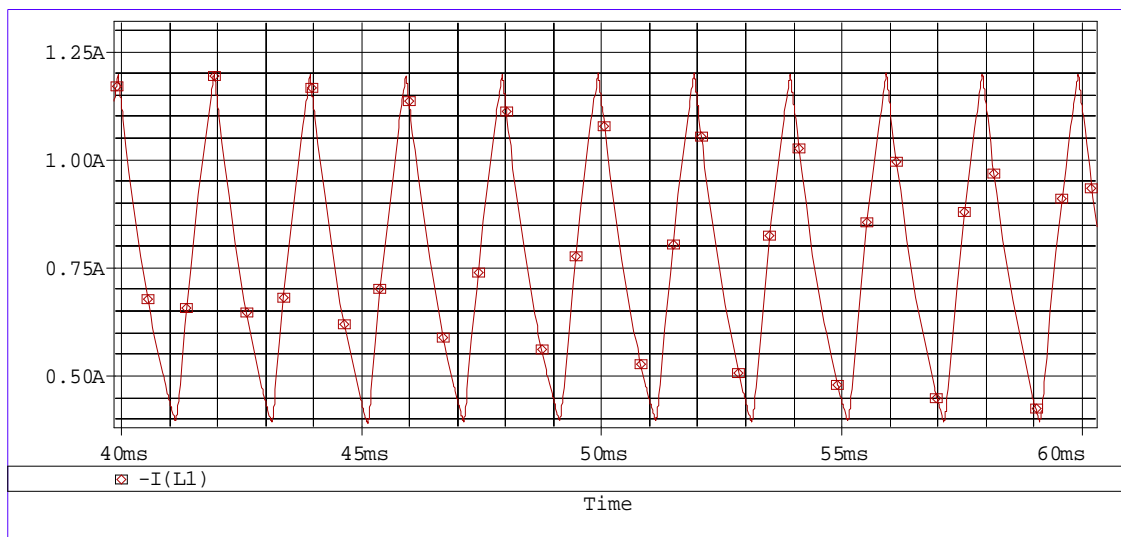


Figure (4-19) Output Current of bidirectional converter

4.3 Bidirectional converter with Battery model results

After modeling and simulating the battery model in the previous section, now this model will be tested as an auxiliary source to the bidirectional converter. The proposed system is shown in figure (4-20). This system was simulated with $R_{\text{batt}}=0.066$, $R_L=7\Omega$ and $K_{\text{Ebatcap}}=0.2$.

Curve in figure (4-21) shows that the waveform of the two transistor Q1 and Q2. A more detailed diagram of the charging process is shown in figure (4-22). It is seen that the battery current is reduced 0.6A, resulting in a reduction of the battery voltage from 8.5 to 5, then the battery voltage rises towards 8.5 because of the battery SOC increase.

The variation in SOC and charge efficiency factor with time is shown in figure (4-23) and figure (4-24). Figure (4-25) shows the relation between charge efficiency and state of charge, while figure (4-26) shows the extracted battery voltage V_{batt} (SOC) the battery voltage increases linearly with the state of charge.

Next, the following figures (4-27) and (4-28) depict the results of the simulation at different temperature for state of charge and charge efficiency respectively.

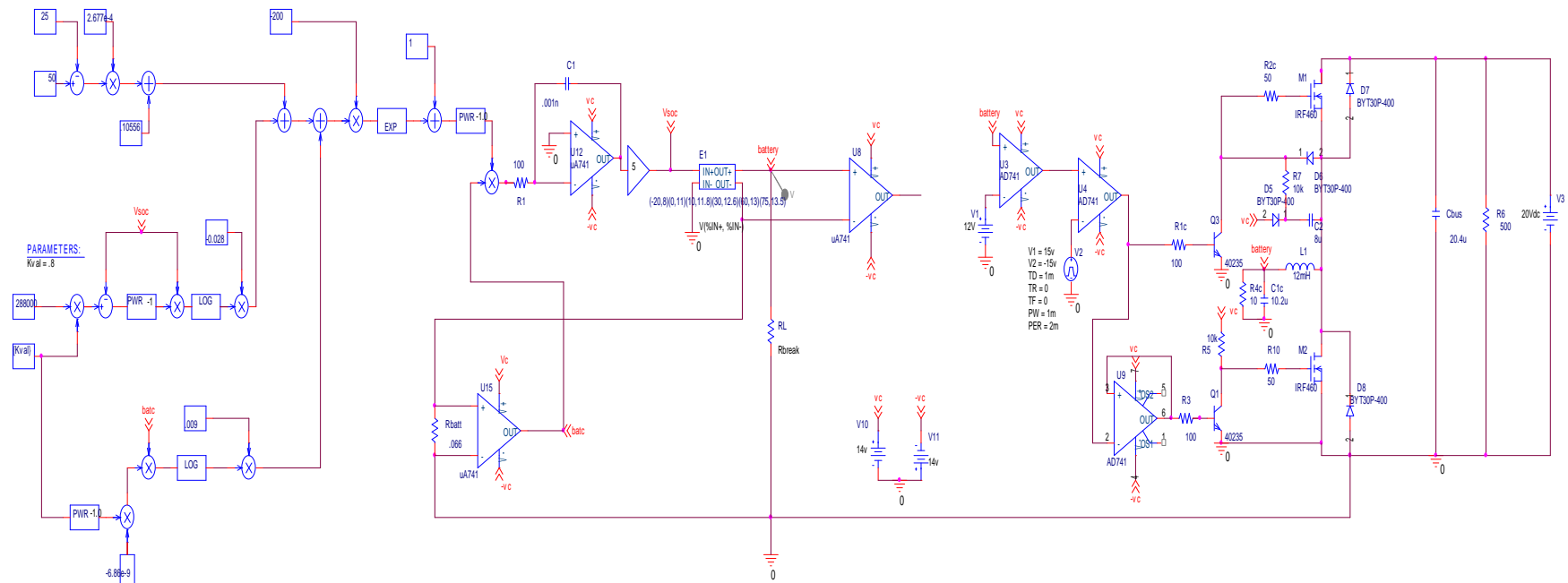
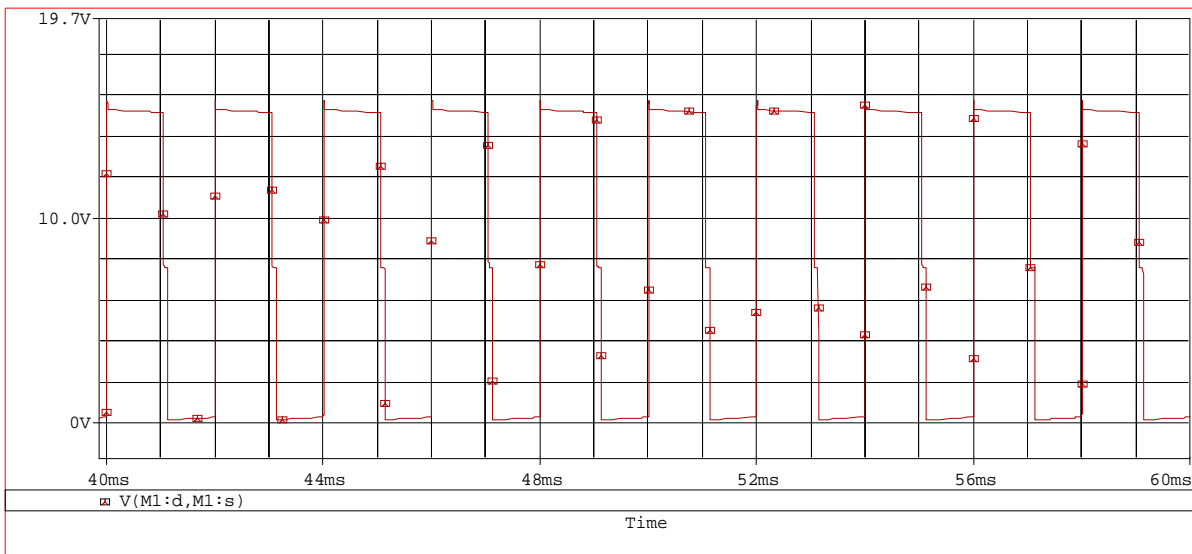
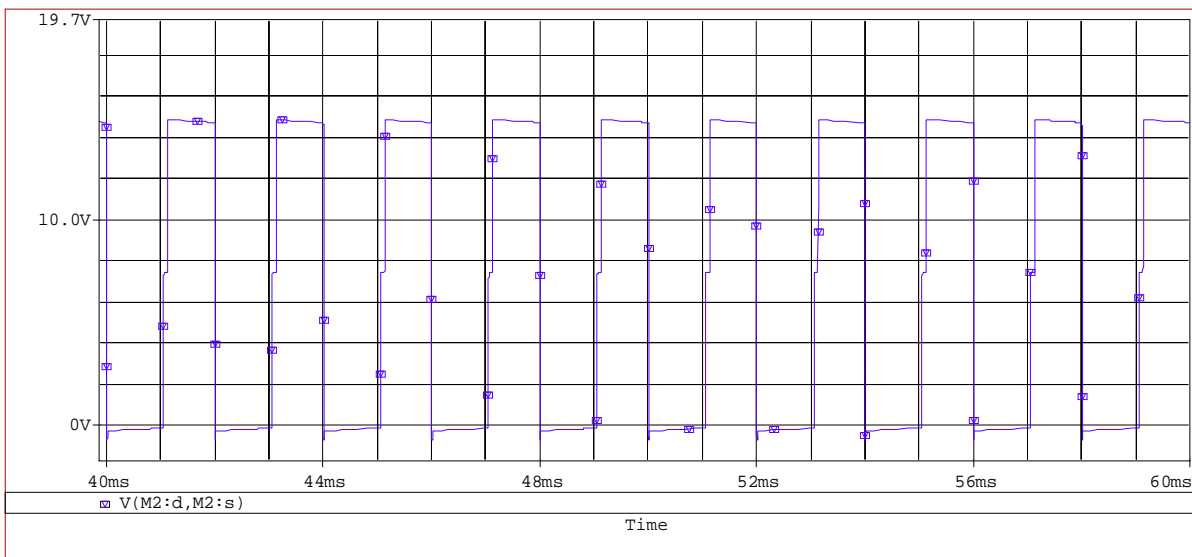


Figure (4-20) total circuit of the battery and converter as represented in PSPICE.



(a)

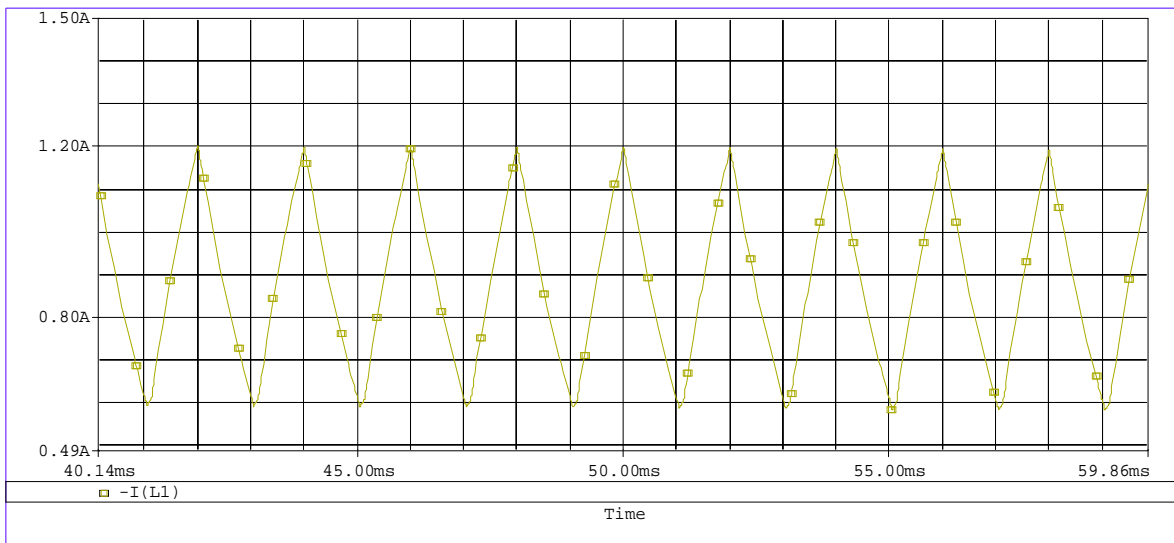


(b)

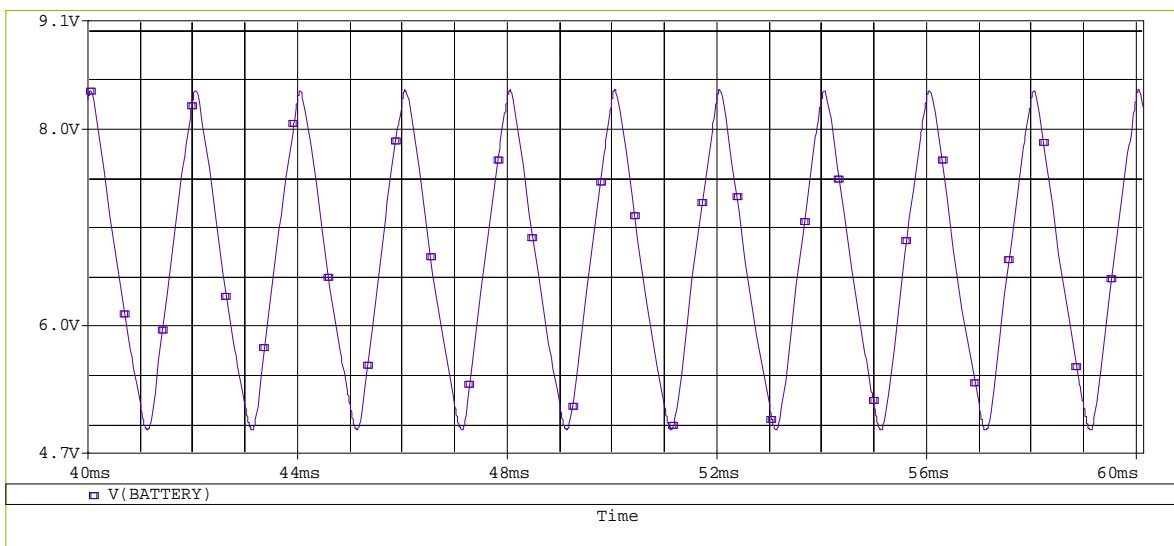
Figure (4-21) voltage as a function of time

(a) Voltage Across M1

(b) Voltage across M2



(a)



(b)

Figure (4-22) current and battery voltage as a function of time

(a) Current

(b) Battery voltage

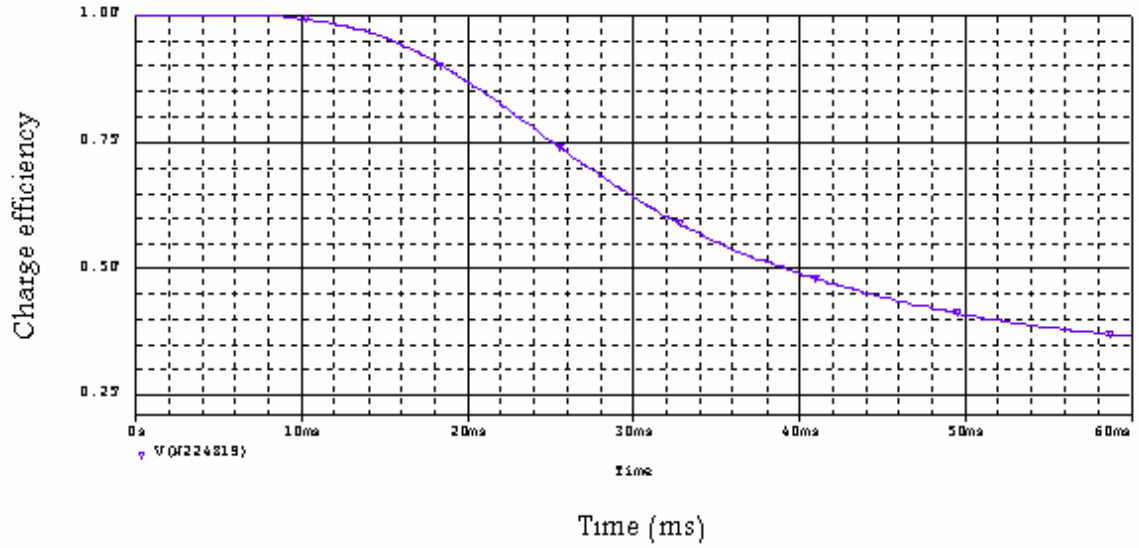


Figure (4-23) charge efficiency as a function of time

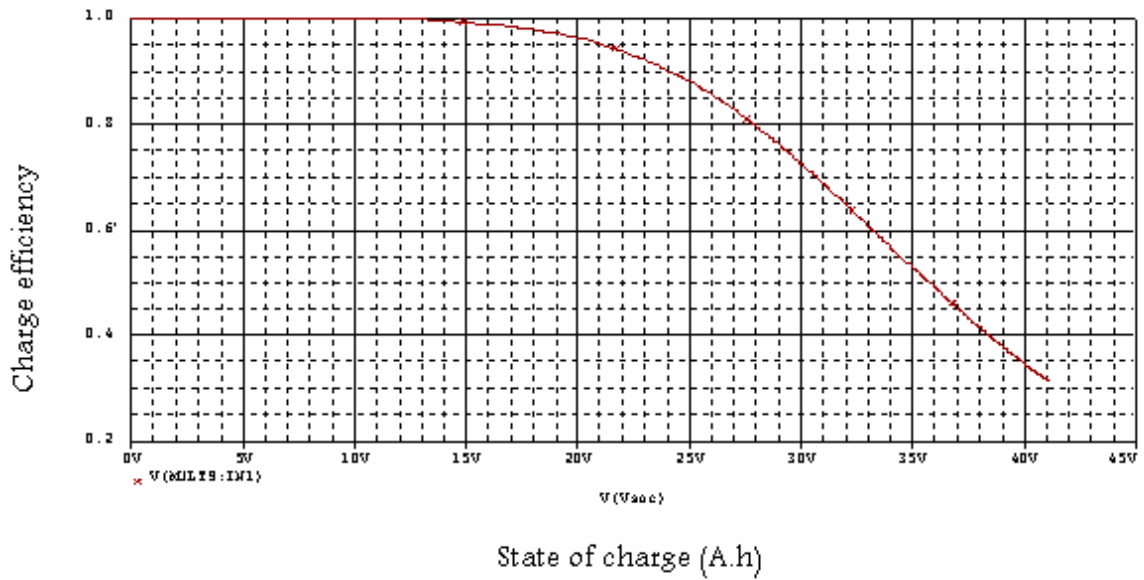


Figure (4-24) charge efficiency as a function of state of charge

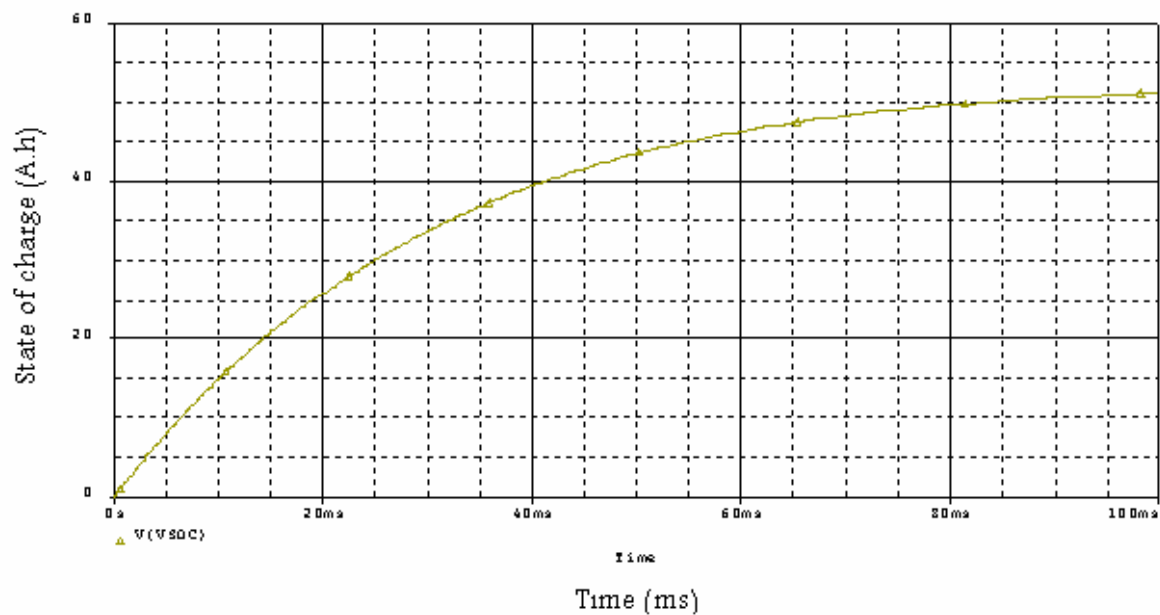


Figure (4-25) state of charge as a function of time

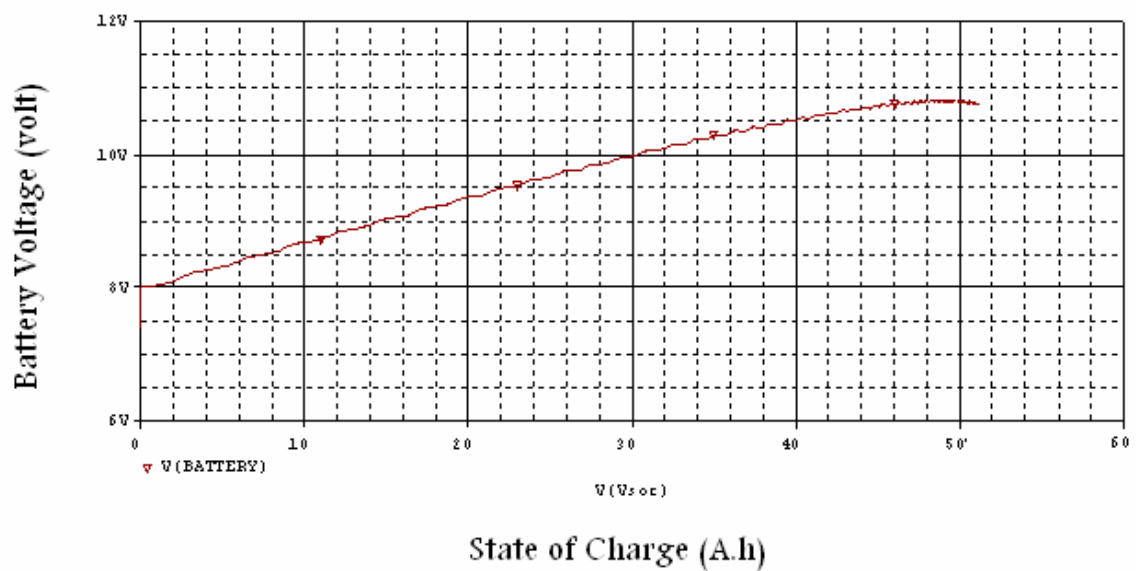


Figure (4-26) battery voltage as a function of state of charge

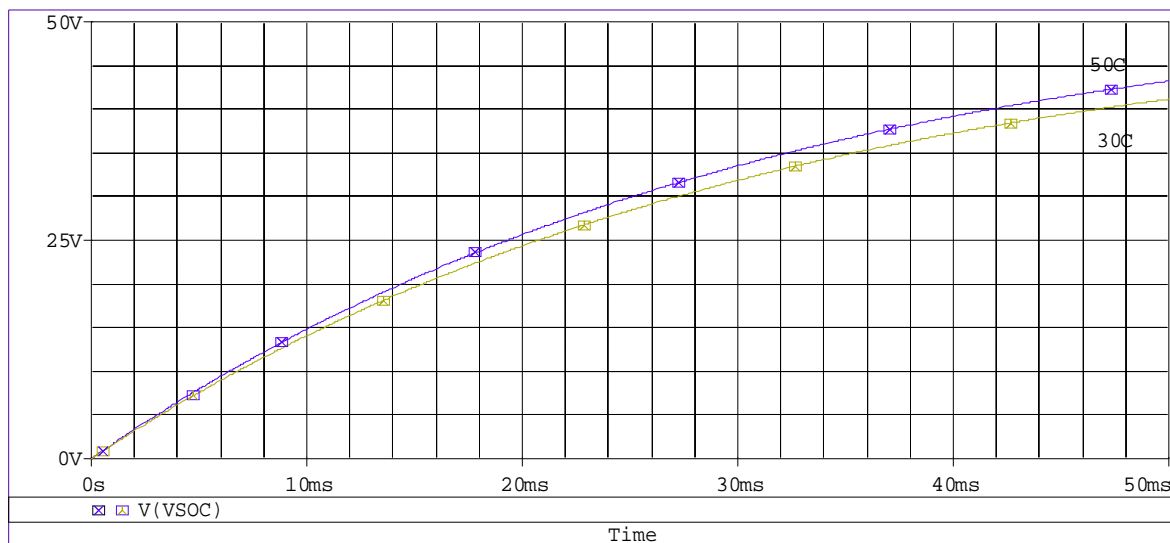


Figure (4-27) state of charge as a function of time at different temperature

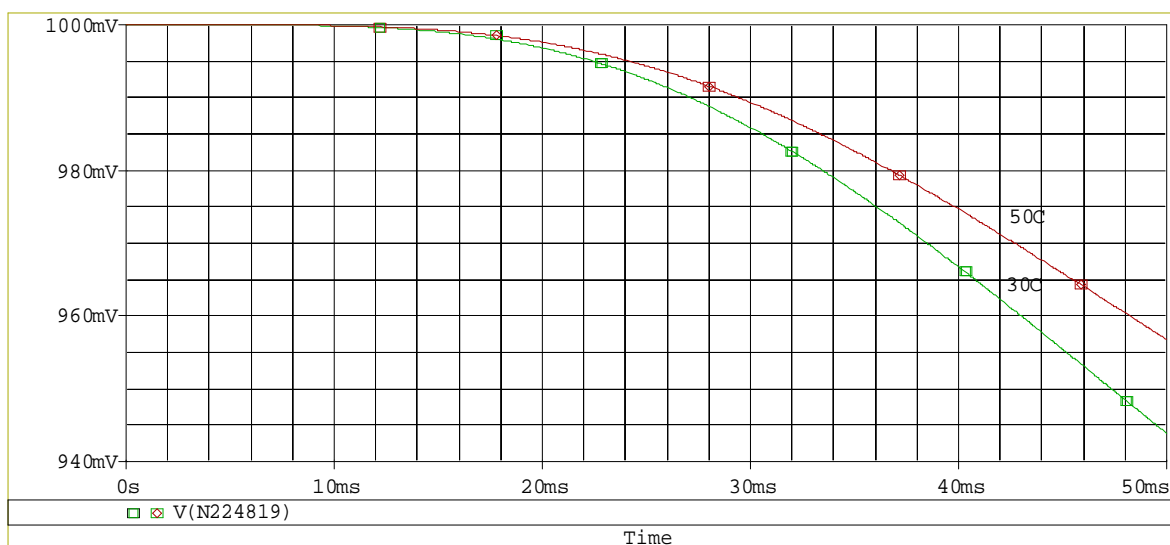


Figure (4-28) charge efficiency as a function of time at different temperature

Chapter
Five

Conclusions
And
Future Work

Chapter Five

Conclusions and Future Work

5.1 Conclusions

Some of the individual achievements and conclusions have been outlined in the following points:

1. An accurate, intuitive and comprehensive electrical model has been proposed to capture the entire dynamic characteristics of a battery, from nonlinear open circuit voltage, SOC and charge efficiency.
2. The model can be used for training personnel in the basic operation of solar energy system or other hybrid systems.
3. A battery model was installed in a Buck-Boost Converter to prove the validity of the battery model.
4. The Buck-Boost Converter was tested with battery and without battery to verify the response and stability of the converter.

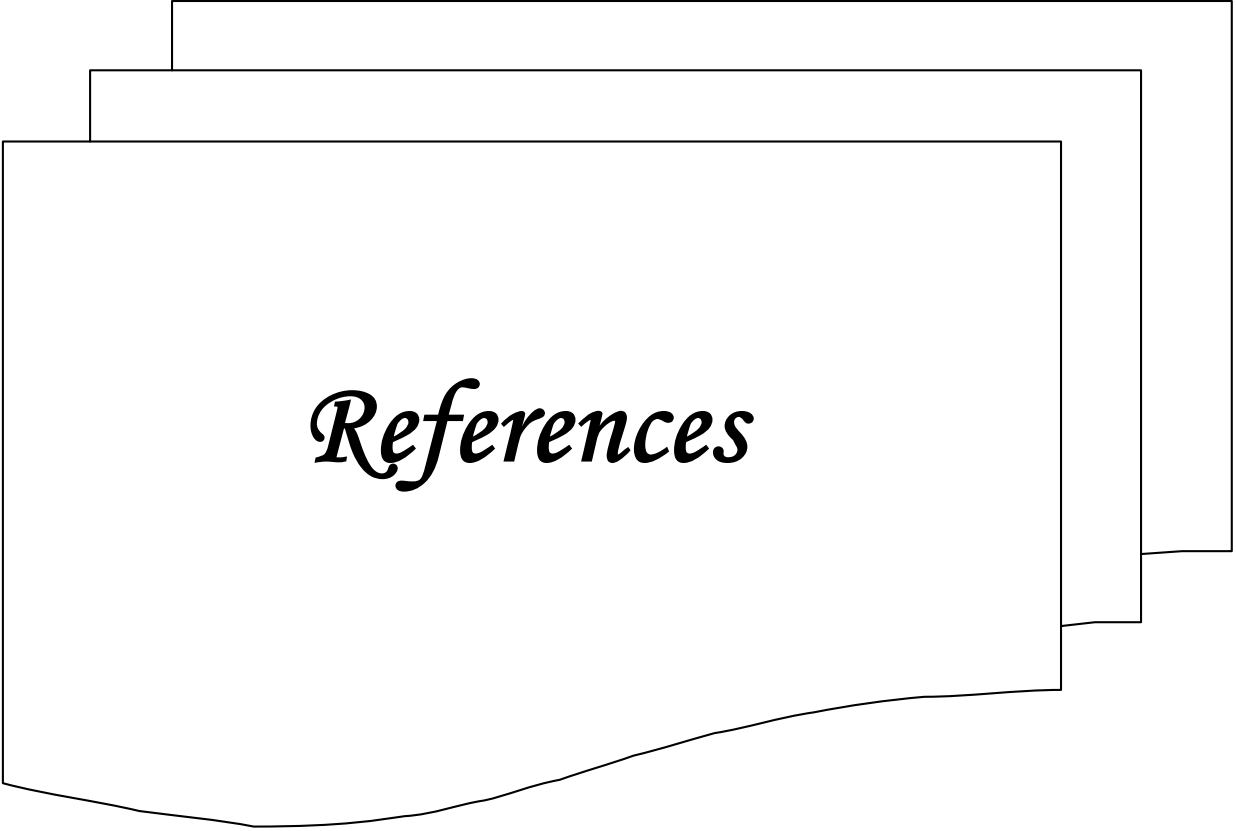
5.2 Future Work

Future work on the frame work would largely depend on the application for which it is being developed however:

1. The battery model which have been implemented have a SOC of positive value and charge efficiency less than one. So, this model could be tested at negative SOC and charge efficiency equal to 1.

2. The control section should be improved, several further features can be developed:
 - Over voltage protection.
 - Battery temperature.

3. The battery model and Bidirectional described in this work could be tested with a PV power source in PSPICE first and then in laboratory.



References

References

Andy M. Mclandrich.

Sensor less control of a bidirectional boost converter for a fuel cell energy management system. August 13, 2003

Battery electricity.

En.Wikipedia.org/Wiki/Battery-(electricity). December 2007.

Chris S., Mike G., Damian U., Andy M., Elton P., and Jih-Sheng L.

Low-Cost solid oxide fuel cell power conditioning with bidirectional charging. IEEE Power Electronics Society, IEEE Industry Applications Society. Fuel Cell seminar, 2003

Espreilla, J.J., Felez, J., Romero, G., and Carretero, A.

A model for simulation a lead-acid battery using bond graphs. Science Direct, simulation modeling practice and theory 15(2007)82-97

Greg Waldo

Pspice Model of the Hubble Space Telescope Electrical Power System
August 19, 2002

Hashem M. Nehrir, Brock J. LaMeres, Giri Venkataramanan, Victor Gerez, and L. A. Alvarado.

An Approach to Evaluate the General Performance of Stand-Alone Wind/Photovoltaic Generating Systems.

IEEE Transactions on energy conversion, vol. 15, no. 4, December 2000.

Haimin T., Andrew K., Jorge D. and Marcel H.

Integration of sustainable energy sources through power electronic converters in small, distributed, electricity generation system.

Technische universiteit eindhoven/ department of electrical engineering electro mechanics and power electronics.

Himmelstoss, F.A., and Wurm, P.A.

Simple bi-directional dc-to-dc converters with high input to output voltage ratio, Technical university Vienna, instate of electrical driven and machines, 16.01.2002

Isidor Buchmann, President.

What is the perfect battery? Cadex Electronics Inc. April 2001

James, P., and Dunlop, P.E.

Batteries and charging control in stand-alone photovoltaic system
Fundamentals and application. Sandia national laboratories, PO Box 5800, Albuquerque, NM 87185- 0752, January 15, 1997

Jinhee lee, Jinsang Jo, Sewarchoi, and Soobin Han

A 10 KW sofc-low voltage battery hybrid power processing unit for residential use. Fuell Cell seminar, 2003

John A. Yoder.

Primer on Lead-acid storage batteries

U.S. Department of Energy Washington, D.C. 20585, September 1995

KADHEM Muter Shiebeeb

Study of formation process of positive plates in Lead-acid Battery.

Department of Chemical Engineering, 1995

Koutroulis, E., and Kalaitzakis, K.

Novel battery charging regulation system for photovoltaic application.

IEE proceedings - Electronic Power appl., vol. 151, No.2, March 2004

Lead-acid battery.

Wikipedia, the free encyclopedia. September 2006

Mohan, N., Undeland, T.M, and Robbins, W.P.

Power electronics converter, application and design second edition.

New York, John Wiley and Sons, 1989

Micah, Q., Juan, D., and Jorge, M.

Design, Construction and performance of a Buck-Boost Converter for an Ultra capacitor-Based Auxiliary energy system for electric vehicles. IEEE

Department of electrical engineering, 2003

Mikael Knunti.

Higher Speed 2kW DC-Dc Converter

Thesis, institution for computer Science and Electronics Malardalens University, 2007.

Sanchis-Kilders, E., Ferreres, A., Maset, E., Ejeat, J.B., Esteven, V., Jordan, J., Garrigo's, A., and Calyente, J.

Soft switching bidirectional converter for battery discharging-charging.

IEEE 2006

Sauradip M., S. K. Sinha, K. Muthukumar.

Estimation of State of Charge of Lead Acid Battery using Radial Basis Function, The 27th Annual Conference of the IEEE Industrial Electronics Society, 2001

Suzanne Foster Porter and Paul Bendt, Ph.D., Ecos Consulting Haresh Kamath and Tom Geist, EPRI Solutions.

Energy Efficiency Battery Charger System Test Procedure, Development funded by: Pacific Gas and Electric and California Energy Commission-Public Interest Energy Research (PIER) Program, March 5, 2008.

Thele, M., Schiffer, J., Karden, E., Surewaard, E., and Sauer, D.U.

Modeling of the charge acceptance of lead-acid batteries. Journal of power sources (2007)

Thomas L.Martin.

Blancing Batteries, power and performance. Ph.D. thesis, Graduate school, Pittsburgh, Pennsylvania, 1999

Tim Robbins and John Hawkins.

Battery model for over-current protection simulation of Dc distribution system. Telstra research laboratories P.O Box 249, Clayton 3168 Australia, 1994 IEEE

Annavajjula V.K

A Failure Accommodating Battery Management System with Individual Cell Equalizers and State Of Charge Observers. Presented to the Graduate Faculty of the University of Akron, December, 2007

Wu, B., Dougal, R., and White, R.E.

Resistive companion battery modeling for electric circuit simulation.
Journal of power sources, 93, pp 186-200 (2001)

Kubba Z.M

Computer aided design and implementation of converter circuits applied
for photovoltaic system. Ph.D. Thesis, 2003

Blue Sky Energy – IPN-ProRemote

This Manual Includes Important Safety Instructions For Models Ipnpro
and Ipnpro-s. Save These Instructions.

www.blueskyenergyinc.com, 2004

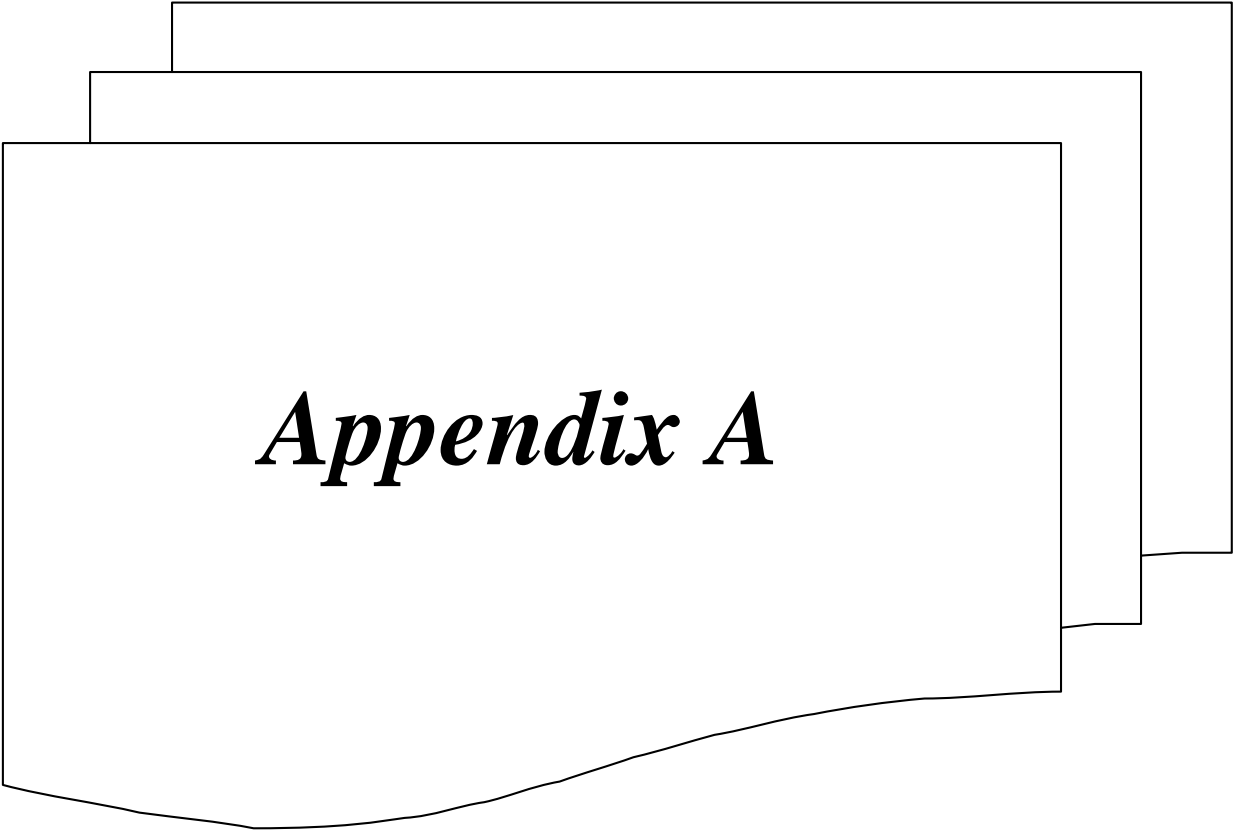
Newsletter list. Newsletter Issue#78, November 2005.

www.intusoft.com/nlhm/n178.htm-52K cached.

Ruffin Rd. and San Diego.

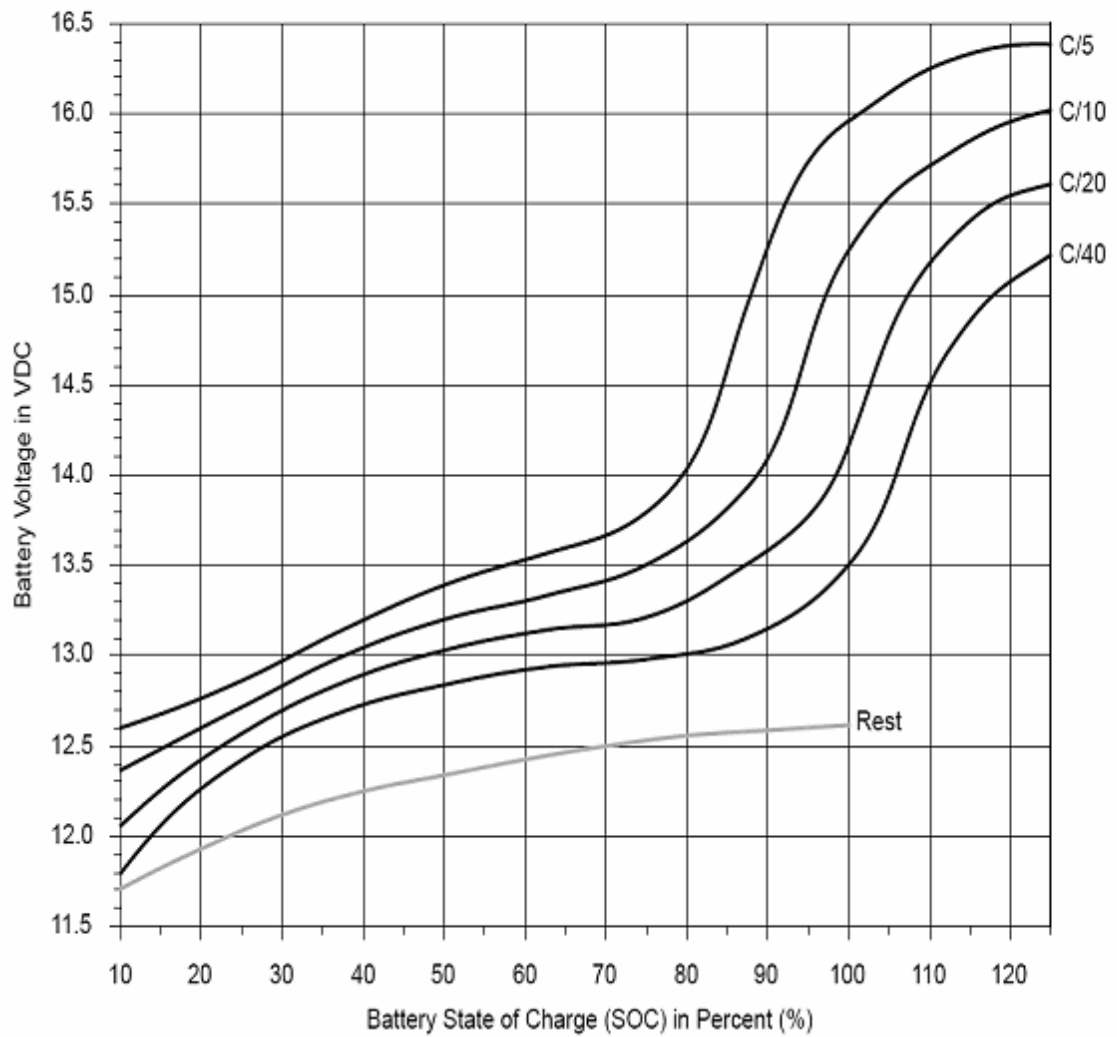
Sea Battery User's Guide P/N 730-001-601.

www.deepsea.com, Rev.5/6/2004

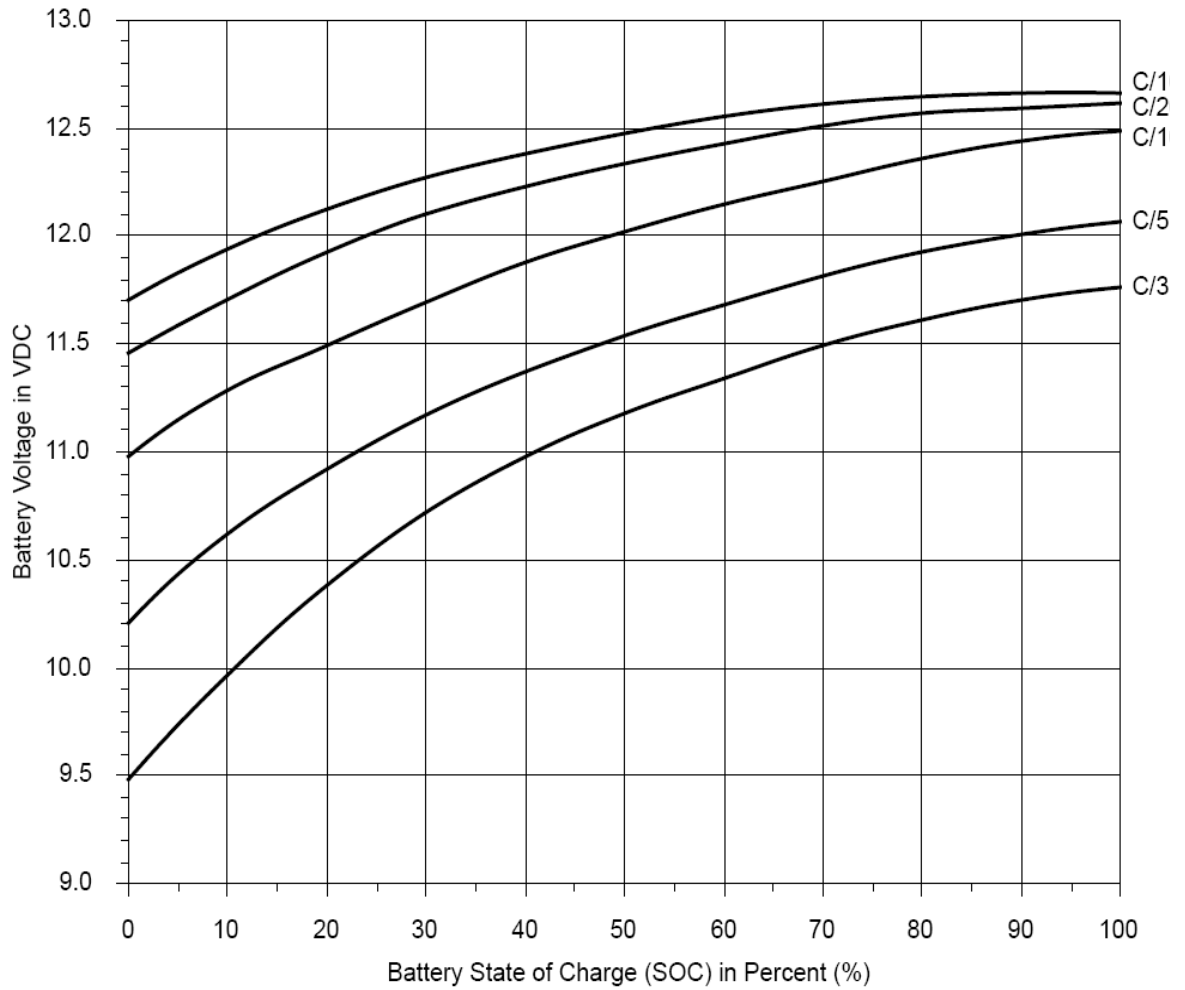


Appendix A

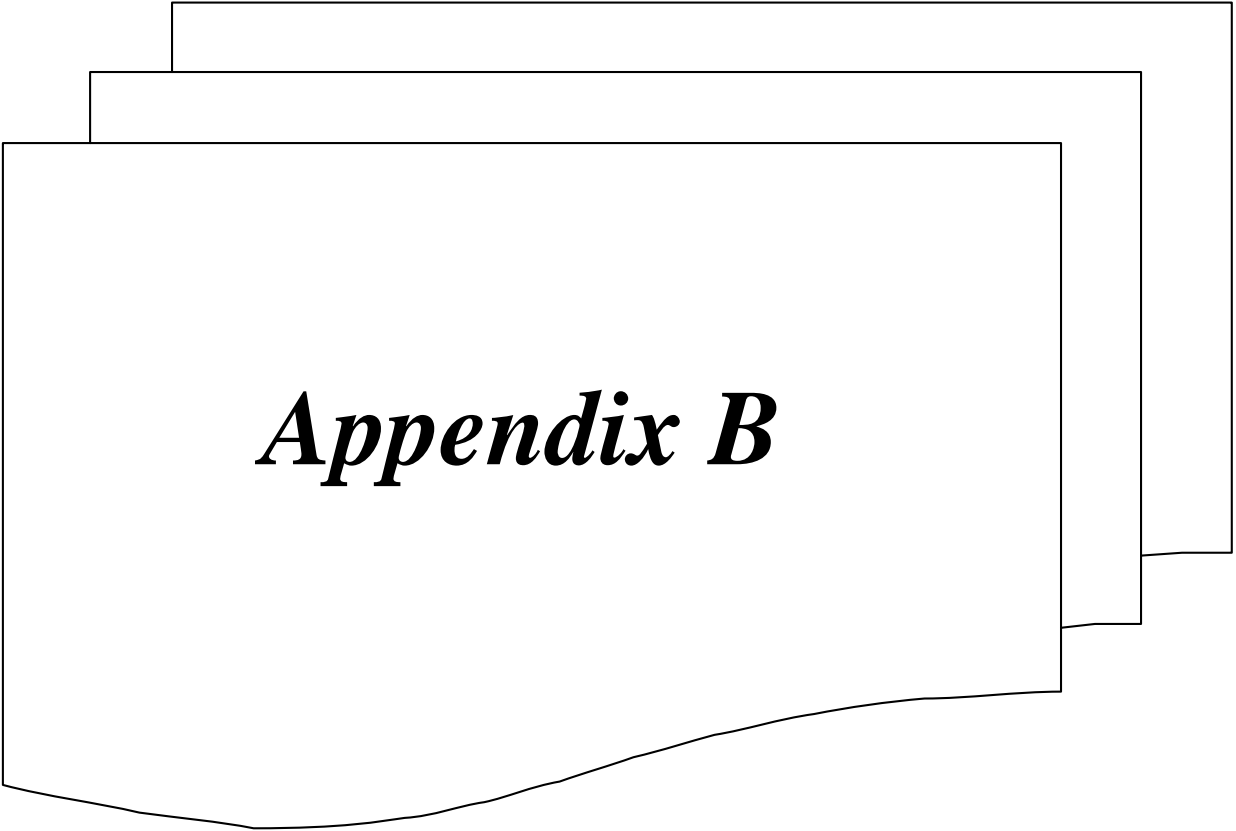
12 Volt Lead Acid Battery State of Charge (SOC) vs. Voltage
while battery is under charge



12 Volt Lead Acid Battery State of Charge (SOC) vs. Voltage while under discharge



Richard Perez
Lead-Acid Battery State of Charge vs. Voltage
August/September 1993



Appendix B

Types of battery

1. Nickel Cadmium (NiCd).

Mature and well understood but relatively low in energy density. The NiCd is used where long life. High discharge rate and economical price are important. Main applications are two-way radios, biomedical equipment, professional video cameras and power tools. The NiCd contains toxic metals and is environmentally unfriendly. [Isidor 2001]

2. Nickel-Metal Hydride (NiMH)

Has a higher energy density compared to the NiCd at the expense of reduced cycle life. NiMH contains no toxic metals. Applications include mobile phones and laptop computer. [Isidor 2001]

3. Lithium Ion (Li-ion)

Fastest growing battery system Li-ion is used where high-energy density and lightweight is of prime importance. The technology is fragile and a protection circuit is required to assure safety. Applications include notebook computer and cellular phones [Isidor 2001].

4. Lithium Ion polymer (Li-Ion polymer)

Offers the attributes of the Li-Ion in ultra-slim geometry and simplified packaging Main applications are mobile phones. [Isidor 2001]

Table (1-1) Battery characteristics [James 1997]

Battery Type	Advantages	Disadvantages
Flooded Lead-Acid		
Lead-Antimony	low cost, wide availability, good deep cycle and high temperature performance, can replenish electrolyte	High water loss and maintenance
Lead-Calcium Open Vent	low cost, wide availability, low water loss, can replenish electrolyte	poor deep cycle performance, intolerant to high temperatures and overcharge
Lead-Calcium Sealed Vent	low cost, wide availability, low water loss	poor deep cycle performance, intolerant to high temperatures and overcharge, can not replenish electrolyte
Lead Antimony/Calcium Hybrid	medium cost, low water loss	limited availability, potential for stratification
Captive Electrolyte Lead-Acid		
Gelled	medium cost, little or no maintenance, less susceptible to freezing, install in any orientation	fair deep cycle performance, intolerant to overcharge and high temperatures, limited availability
Absorbed Glass Mat	medium cost, little or no maintenance, less susceptible to freezing, install in any orientation	fair deep cycle performance, intolerant to overcharge and high temperatures, limited availability
Nickel-Cadmium		
Sealed Sintered-Plate	wide availability, excellent low and high temperature performance, maintenance free	only available in low capacities, high cost, suffer from 'memory' effect
Flooded Pocket-Plate	excellent deep cycle and low and high temperature performance, tolerance to overcharge	limited availability, high cost, water additions required

الخلاصة

يهدف هذا البحث الى تصميم مغير ثنائي الاتجاه المستخدم في العديد من التطبيقات ومنها الخلايا الشمسية ونظام شحن وتفريغ البطارية باستخدام مجهز قدرة اضاقي، وقد تم تحقيق ذلك باستخدام برنامج التحليل PSPICE.

تم تصميم موديل لبطارية (12V) Lead Acid المستخدمة في الكثير من التطبيقات. يتكون الموديل من كفاءة الشحن و مكونات فولطية البطارية. تتراوح قيمة عامل كفاءة الشحن بين (صفر الى واحد) ويعتمد على حالة الشحن والتيار الشاحن. تتشكل مكونات فولطية البطارية من Etable, Integrator. طبق هذا الموديل ايضا في برنامج PSPICE مع المغير الثنائي الاتجاه ذو المواصفات التالية ($D=0.4$ ، $P=12W$ ، $V_o=12V$ ، $f_s=1\text{ KHz}$ ، $I_o=1A$)، وتم اثبات صحة هذا الموديل من خلال النتائج المستحصلة وكانت متفقة مع الواقع العلمي.



جمهورية العراق
وزارة التعليم العالي و البحث العلمي
جامعة النهرين
كلية العلوم
قسم الفيزياء

نموذج بطارية باستخدام برامجيات

PSPICE مع مغير شحن ثنائي

الاتجاه

رسالة

مقدمة إلى كلية العلوم في جامعة النهرين وهي جزء من متطلبات نيل
درجة الماجستير في

الفيزياء

من قبل

زينة موفق قدوري العزاوي

(بكالوريوس ٢٠٠٤)

بإشراف

د. زينب منذر يونس كبة

في

١٤٢٩هـ

٢٠٠٨م

شوال

تشرين الاول